I.O.S.

Fil.

WAVES AT SEVEN STONES LIGHT VESSEL
(50° 04'N, 06° 04'W)

January 1968 to June 1974

by

B. C. H. FORTNUM and H. M. TANN

Report No 39

1977

NATURAL ENVIRONMENT RESEARCH COUNCIL

INSTITUTE OF OCEANOGRAPHIC SCIENCES

INSTITUTE OF OCEANOGRAPHIC SCIENCES

Wormley, Godalming,
Surrey, GU8 5UB.
(0428 - 79 - 4141)

(Director: Professor H. Charnock)

Bidston Observatory,
Birkenhead,
Merseyside, L43 7RA.
(051-653-8633)
(Assistant Director: Dr. D. E. Cartwright)

Crossway,
Taunton,
Somerset, TA1 2DW.
(0823-86211)
(Assistant Director: M.J. Tucker)

Marine Scientific Equipment Service
Research Vessel Base,
No. 1 Dock,
Barry,
South Glamorgan, CF6 6UZ.
(04462-73451)
(Officer-in-Charge: Dr. L.M. Skinner)

WAVES AT SEVEN STONES LIGHT VESSEL

($50^{o}04'N, 06^{o}04'W$)

January 1968 to June 1974

by

B C H FORTNUM and H M TANN

The preparation of this report and the collection of some of the data contained in it have been financed by the Departments of Energy and of Industry

Report No 39

1977

Institute of Oceanographic Sciences
Crossway
Taunton
Somerset

CONTENTS

CONTENTS (continued)

Figure Captions:

Map to show location of Seven Stones Wave Recorder

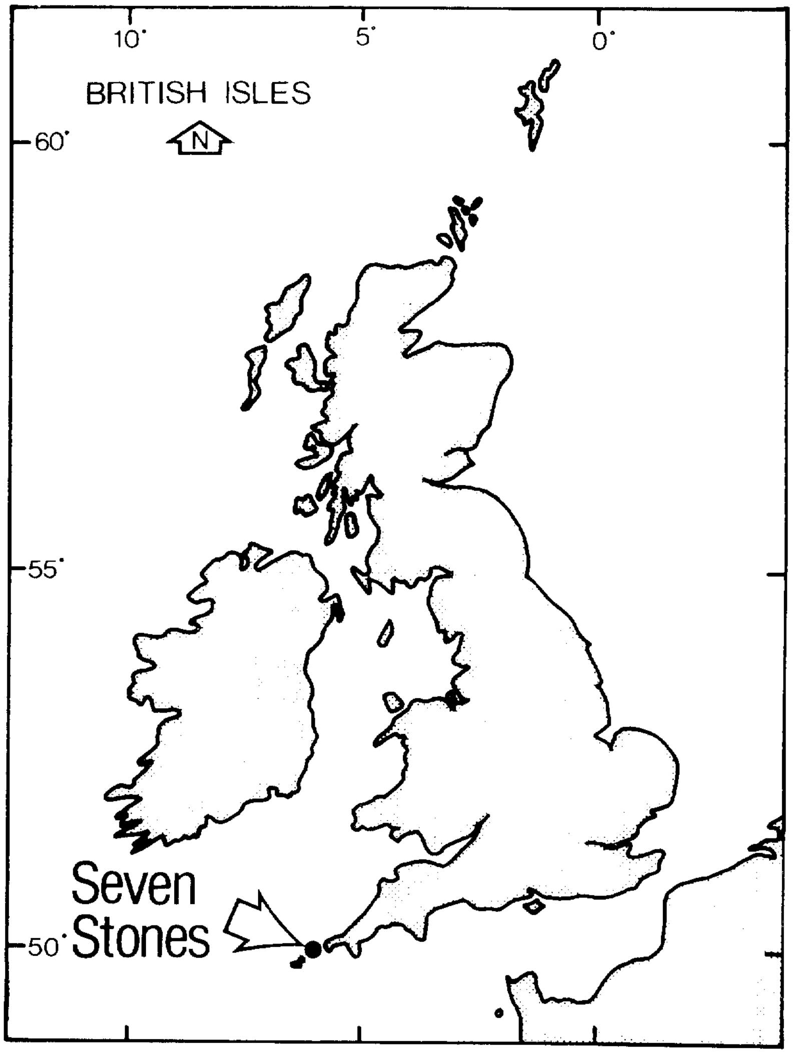

INTRODUCTION

The Institute of Oceanographic Sciences and its forerunner, the National Institute of Oceanography, have measured waves at Seven Stones Light Vessel since 1962. A summary of the data from the first year of operation has been given by Draper and Fricker (1965). The present report gives an analysis of the measurements taken from January 1968 to June 1974.

Seven Stones Light Vessel marks the position of the Seven Stones rocks, and is moored in about sixty metres of water at a location approximately seventeen kilometres north east of the Scilly Isles (see figure at the beginning of this report). The site is open to winds which blow across the Atlantic Ocean, so that it is the most exposed of the Trinity House light vessel stations.

The light vessel is fitted with a shipborne wave recorder (see Tucker, 1956) maintained by the Institute of Oceanographic Sciences. Twelve-minute samples of the variation of surface elevation are taken every three hours and recorded on paper chart rolls.

The instrument can only be calibrated when the ship docks for refit, which occurs once every three years, although regular testing in between these calibrations will detect any major malfunction which occurs. Calibrations were carried out during October-November 1967 and April-May 1971. Data from the third year after calibration are not considered usable because after that period there is a risk that marine growth will obstruct the tube through the hull which leads to the pressure sensor. Accordingly, the data considered reliable and analysed in this report consist of the five complete twelve-month periods shown below.

Period		% valid data
January 1968 to December 1968		99.8
January 1969 to December 1969		97.7
July 1971 to June 1972		99.5
July 1972 to June 1973		99.0
July 1973 to June 1974		99.7
	Average:	99.1

METHODS OF ANALYSIS

The technique used to analyse the wave data was that proposed by Tucker (1961) and Draper (1963) and reviewed by Tann (1976). For each three-hour interval the corresponding twelve-minute record gives values of the following parameters.

1. The number of zero up-crossings, N_z. A zero up-crossing is considered to occur when the trace crosses the mean line in an upward direction.

2. The number of crests, N_c.

3. The mean zero up-crossing period, T_z. This is defined as the duration of the record divided by N_z.

4. The standard deviation, σ.

5. The significant wave height, H_s. This is defined as 4σ. For a narrow band random process this parameter approximates closely to the mean height of the highest one-third zero up-cross waves (Longuet-Higgins (1952)). Comparison between the two definitions is made by Goda (1970, 1974). (A zero up-cross wave is defined as the portion of the wave record between two zero up-crossings, and its height is the vertical distance between the highest and lowest points on the wave.)

6. The most probable height of the highest zero up-cross wave in the three-hour interval, H_{max} (3 hr).

7. The bandwidth parameter, ε, which is a measure of the range of frequencies present. $\varepsilon = \sqrt{1 - \left(\frac{N_z}{N_c}\right)^2}$

The parameter H_{max} (3hr), which is the mode of the distribution, should not be confused with the expected height of the highest wave in three hours, which is the mean of the distribution. The mean of the distribution is typically 3% higher than the mode (Tann (1976)).

This method of analysis introduces statistical scatter leading to a standard error of 6% in the abstracted wave height parameters (Tann (1976)). It is of little importance in the majority of applications, but when extrapolating the long-term cumulative distribution of wave heights (Figures 23 to 27) it is important that the large values are estimated as accurately as possible. To ensure this, the records giving the twenty-three largest values of significant wave height were digitized and new values of H_S and H_{max} (3 hr) were obtained from the computed root-mean-square surface elevation.

Mathematical formulae for the four cumulative distributions used for H_{max} (3hr) in this report are:

1. Weibull

$$\mathrm{Prob}(X \leqslant x) = \begin{cases} 1-\exp\left[-\left(\frac{x-A}{B}\right)^C\right], & \text{for } x > A \\ 0 & \text{, for } x \leqslant A \end{cases}$$

where B and C are positive, and A represents a lower bound on H_{max} (3hr).

2. Log-Normal

$$\mathrm{Prob}(X \leqslant x) = H\left(\frac{\ln x/\beta}{\delta}\right)$$

where H is the normal distribution function

$$H(\Theta) = \frac{1}{\sqrt{2\pi}}\int_{-\infty}^{\Theta} \exp\left(\frac{-t^2}{2}\right) dt.$$

3. Gumbel's Third Asymptote

$$\mathrm{Prob}(X \leqslant x) = \begin{cases} \exp\left[-\left(\frac{A-x}{B}\right)^C\right], & \text{for } x \leqslant A \\ 1 & \text{, for } x > A \end{cases}$$

where B and C are positive. This is the extreme value distribution first considered by Fisher and Tippett (1928) for a variable bounded above by A (see Gumbel (1958)). Letting this bound tend to infinity gives the first asymptotic distribution, as below.

4. Gumbel's First Asymptote

$$\mathrm{Prob}(X \leqslant x) = \exp\left[-\exp(-ax+b)\right].$$

DISCUSSION OF RESULTS

The division of the year into four three-monthly seasons was made on the basis of Figure 28. By examining the magnitudes of the mean values of H_S for each month, the most obvious grouping of the months into seasons is:

Spring	March, April, May
Summer	June, July, August
Autumn	September, October, November
Winter	December, January, February

FIGURES 1 to 4. Percentage exceedance of H_s and H_{max} (3hr).
These graphs may be used to estimate the fraction of the time during which H_s or H_{max} (3hr) exceeds a given height. For instance, from Figure 1 we see that during spring the significant wave height exceeded four metres 9.5% of the time.

FIGURES 5 to 8. Frequency Histograms for T_z.
It is noticeable that wave periods were largest in the winter, while in summer there was a particularly large number of occurrences of zero-crossing period near seven seconds.

FIGURES 9 to 13. Scatter diagrams.
The numbers of occurrences of particular pairs of values of significant wave height and zero-crossing period, expressed in parts per thousand, are shown in these diagrams. Joining up points with equal numbers of occurrences as shown ('contouring') gives a representation of the bivariate probability distribution and illustrates the correlation between H_s and T_z. Theoretically, the limiting value of wave steepness for a progressive wave is 1:7, where wave steepness is defined as the ratio of wave height to wave length. However, both significant wave height and zero-crossing period are average quantities and on the scatter diagrams for these two quantities there is a fairly well defined limit of about 1:13. (Steepness is defined for this purpose as $\frac{2\pi H_s}{g T_z^2}$.)

A scatter diagram gives a good description of the character of the wave climate, so a scatter diagram for the whole year has been included for comparison with other locations.

FIGURE 14. Frequency histogram for ε .
Values of ε between 0.5 and 0.7 are most common, with a 20% change in the most frequent value from summer to winter.

FIGURES 15 to 22. Persistence diagrams.

Use of the terms 'storm' and 'calm' is illustrated in the following example: a six-metre calm (storm) is said to occur when the significant wave height is less (greater) than six metres. Given a duration D hours, a diagram of persistence of calms (storms) shows how many calms (storms) with duration greater than or equal to D hours can be expected during the season in question.

For example, suppose an operator requires twelve hours with H_s smaller than three metres to complete a particular job. It may be seen from Figure 16 that there will be on average nine occasions during the summer when the job may be done. As an example of the use of the diagrams for persistence of storms, suppose a supply vessel cannot unload onto a platform when the significant wave height exceeds three metres. It may be seen from Figure 22 that there will be on average three occasions during the winter when the vessel would have to wait more than 96 hours to unload.

FIGURES 23 to 27. Cumulative distribution of H_{max} (3 hr).

The cumulative distribution of H_{max} (3 hr) for the whole period covered by this report is plotted on four scales as shown and a straight line fitted where appropriate. This is equivalent to fitting the corresponding distribution function to the data. Having found the distribution which gives a satisfactory fit, the line is extrapolated to find heights which have a very low probability of being exceeded.

It would be misleading to fit a straight line to the data in Figure 24 (the log-normal plot) since the data clearly deviate significantly from a log-normal distribution at the higher wave heights.

A value of 1.3m for the lower bound, A, was found to produce the best alignment of data points for the Weibull distribution (Figure 23).

For Gumbel's Third Asymptotic distribution (Figure 26), both the position of the line and the value of 55m for the upper bound, A, were chosen to give a least-squares best fit.

Visual inspection of the four graphs shows that this latter distribution follows the data best, and from this distribution the height of the wave with a 50-year return period is found to be 23.4m. Comparable results from the Weibull distribution and Gumbel's First Asymptotic distribution are 23.7m and 25.1m respectively. Confidence limits of 70% have been drawn about the extrapolated part of the regression line in Figure 26 (Gumbel's Third Asymptotic distribution). The confidence limits represent an equal probability of the extreme wave height lying either side of the regression line, although on the scales shown this requires the confidence intervals above and below the regression line to be of unequal widths. At the probability corresponding to the 50-year return period, the upper and lower 70% confidence limits are 25.8m and 22.6m respectively.

The maximum value of H_{max}(3 hr) for each of the five twelve-month periods is also plotted as a cumulative distribution, using Gumbel's Third Aymptotic distribution with the upper bound, A, equal to 55m (Figure 27). Using a least squares regression analysis, the value of the 50-year extreme wave height from this distribution is found to be 24.6m, showing only a 5% difference from the value obtained using all the values of H_{max}(3 hr) (Figure 26).

It should be realised that the 50-year extrapolated value of H_{max}(3 hr) is not quite the same as the most probable height of the highest wave in fifty years. Correlation between successive values of H_{max}(3 hr) has been ignored, as has the fact that the largest wave might occur when H_{max}(3 hr) is not at its maximum. The errors contributed by these two effects have been roughly estimated under certain assumptions to be −2.3% and +6% respectively (Tann (1976)). Thus assuming the 50-year storm has duration twelve hours, the most likely height of the largest wave in fifty years will typically be 3½% higher than the 23.4m quoted above.

FIGURE 28. Month-to-month variability of significant wave height.
The average value of significant wave height for each of the sixty months of data is calculated and for each of the months from January to December, the mean and standard deviation of the five averages are plotted.

January was found to have a large standard deviation of 21%, due mainly to a particularly large average H_s for January 1974 of 4.98m. On the other hand the average value of H_s for the summer months of June, July and August varied little throughout the period covered by this report.

FIGURES 29 to 34. Year-to-year variability of significant wave height.

The year-to-year variability of wave conditions is illustrated in two ways. Figure 29 shows the mean of the N largest values of H_s, for the given year, for N = 1, 5, 10, 20, 50, 100. Figures 30 to 34 show the cumulative distribution of H_{max}(3 hr) plotted on scales on which Gumbel's First Asymptotic distribution would appear as a straight line, as in Figure 25. A least-squares regression analysis performed on each of the twelve-month data sets gives the following heights for the 50-year wave:

1968	24.4m
1969	24.4m
1971/72	27.5m
1972/73	24.7m
1973/74	28.8m

These wave heights have a mean of 26.0m and a range of 4.4m, which is 16.9% of the mean. The danger of extrapolating to design heights from just one year's data is quite apparent from these figures.

WIND DATA

The wave data at Seven Stones cover a period of five years, whereas wind data are available for fifteen years. These wind data may indicate how representative wind conditions were between 1968 and 1974 in the vicinity of Seven Stones. This in turn may be taken as an indication of how representative the wave data described in this report are for the Seven Stones location.

The wind data used were from the station Scilly ($46^{\circ}56'$N, $06^{\circ}18'$W), and cover the period from 1960 to 1975. Winds approaching the site from Cornwall will affect the wave conditions significantly less than those from other directions because of the limitations of fetch, and they have not been considered (ie winds from directions 050° to 100° inclusive have been excluded from this analysis). The data are in the form of three-hourly synoptic values, with the exception of the year 1972/73, during which no data were available for five of the winter months. Consequently for that twelve-month period, one-hourly anemograph values have been substituted, a 10% reduction having been made in them to correct them to a nominal effective height of 10 metres.

FIGURE 35. Month-to-month variability of wind speeds.

This figure shows the mean and the standard deviation of the average wind speeds for each month; data both for the years covered by this report and for the full fifteen years are shown. It can be seen that, for every month of the year, the mean wind speed for each month for the years 1968 to 1974 is less than the corresponding mean wind speed calculated for the years 1960 to 1975.

FIGURE 36. Year-to-year variability of wind speeds.
For each twelve-month period shown, the mean of the highest N values of wind speed is plotted, for N = 1, 5, 10, 20, 50, 100. The figure shows that the maximum wind speeds recorded during 1968 to 1974 lie approximately in the middle of the range of maximum wind speeds recorded during the fifteen years from 1960 to 1975. On this basis, the wind conditions, and therefore the wave conditions also, may be considered to be fairly representative for the location during the years 1968 to 1974.

ACKNOWLEDGEMENTS

The authors are grateful to the many people whose contributions have made it possible to produce this report. In particular, the Elder Brethren of Trinity House for permission to install the shipborne wave recorder in the Seven Stones Light Vessel, the Master and crew of the Seven Stones Light Vessel for operating the equipment, Mr L Draper for the installation of the equipment and Mr F Wardle for maintaining and re-calibrating it, both of the Institute of Oceanographic Sciences, and Mr D J Painting of the Meteorological Office for supplying the wind data.

REFERENCES

DRAPER L 1963. Derivation of a 'design wave' from instrumental records of sea waves. Proceedings of the Institution of Civil Engineers 26, 291-304.

DRAPER L and FRICKER H S 1965. Waves off Land's End. Journal of the Institute of Navigation 18, No 2, 180-187.

FISHER R A and TIPPET L H C 1928. Limiting forms of frequency distribution of the largest or smallest member of a sample. Proceedings of the Cambridge Philosophical Society 24, 180-190.

GODA Y 1970. Numerical experiments on wave statistics with spectral simulation. Report of the Port and Harbour Research Institute 9, No 3, 3-57.

GODA Y 1974. Estimation of wave statistics from spectral information. Proceedings of the International Symposium on Ocean Wave Measurement and Analysis, 320-337.

GUMBEL E J 1958. Statistics of Extremes. New York: Columbia University Press. 371 pp.

LONGUET-HIGGINS M S 1952. On the statistical distribution of the heights of sea waves. Journal of Marine Research 11, No 3, 245-266.

TANN H M 1976. The estimation of wave parameters for the design of offshore structures. Institute of Oceanographic Sciences, Report No 23.

TUCKER M J 1956. A shipborne wave recorder. Transactions of the Institution of Naval Architects 98, 236-250.

TUCKER M J 1961. Simple measurement of wave records. Proceedings of the Conference on Wave Recording for Civil Engineers, National Institute of Oceanography, 22-23.

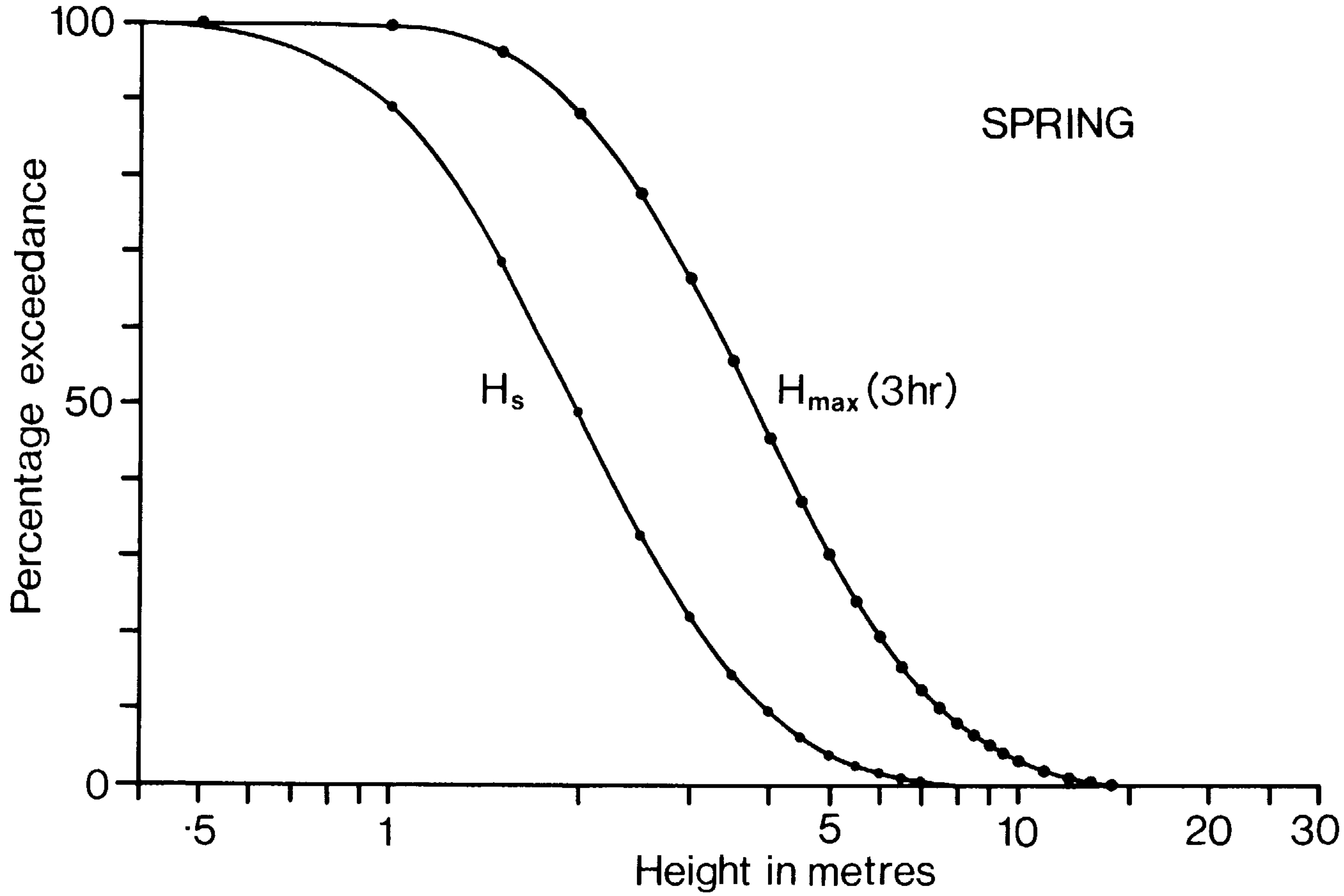

Percentage exceedance of H_s and H_{max} (3hr) - Spring

Fig. 1

SS

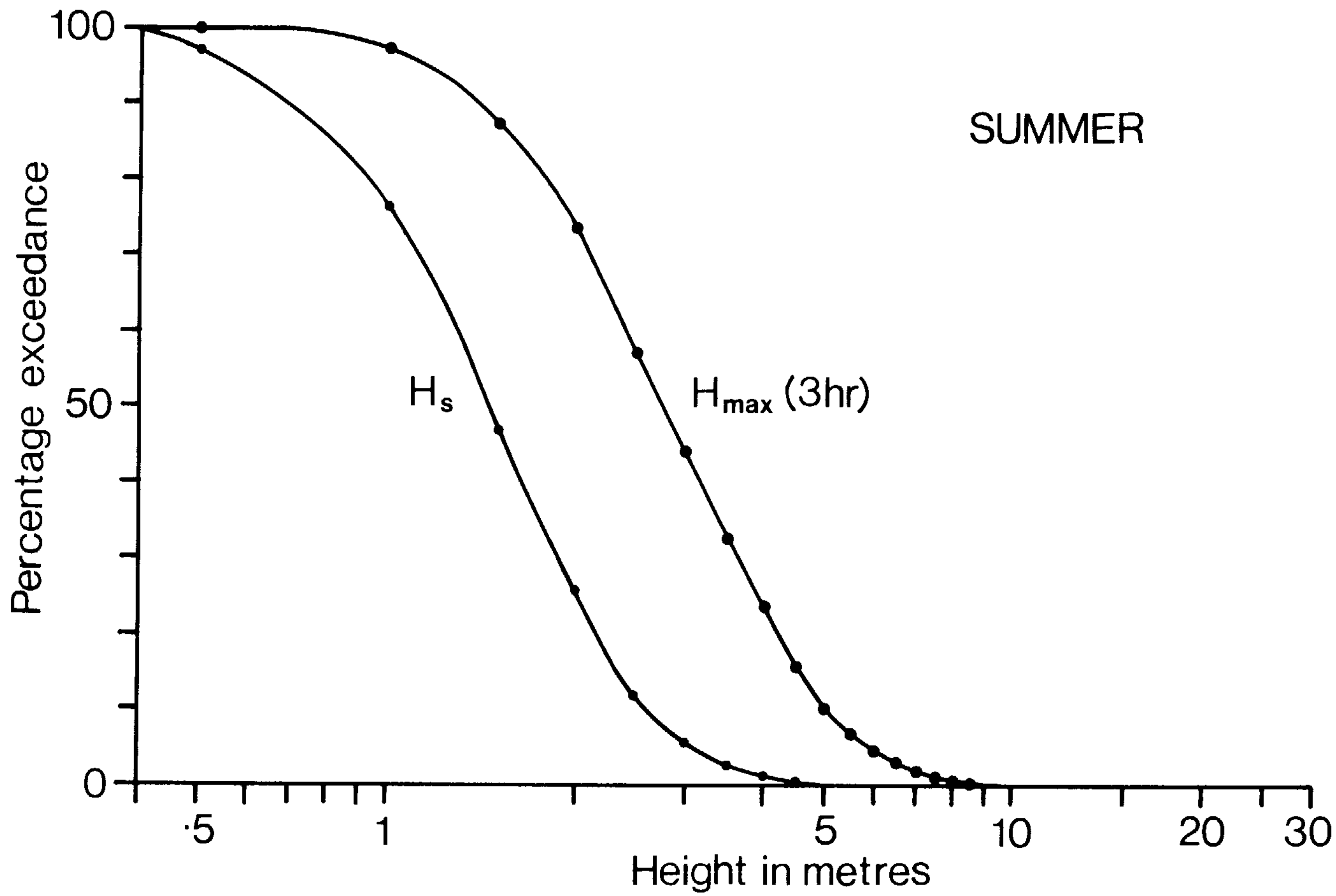

Percentage exceedance of H_s and H_{max} (3hr) - Summer

Fig. 2

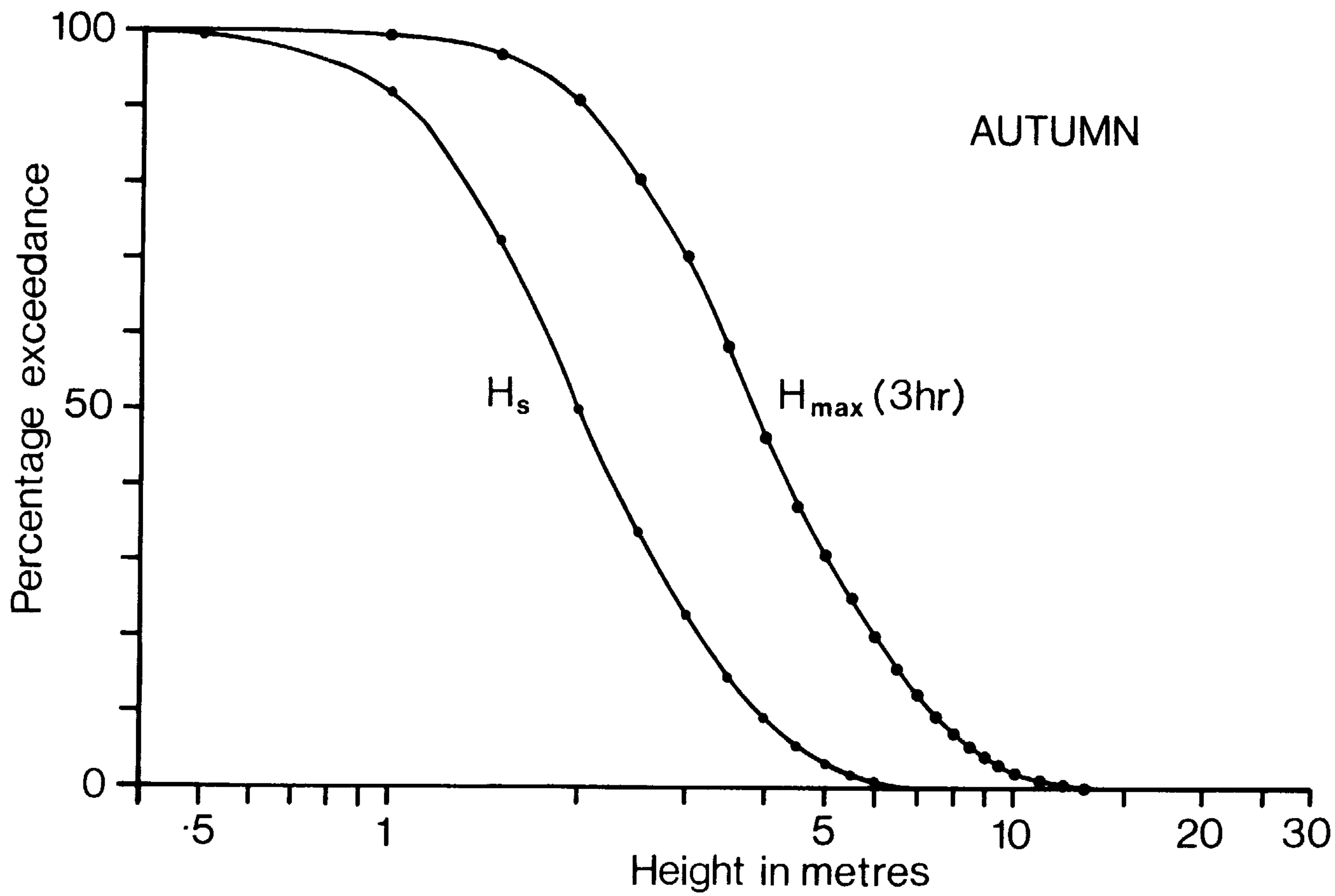

Percentage exceedance of H_s and H_{max} (3hr) - Autumn

Fig. 3

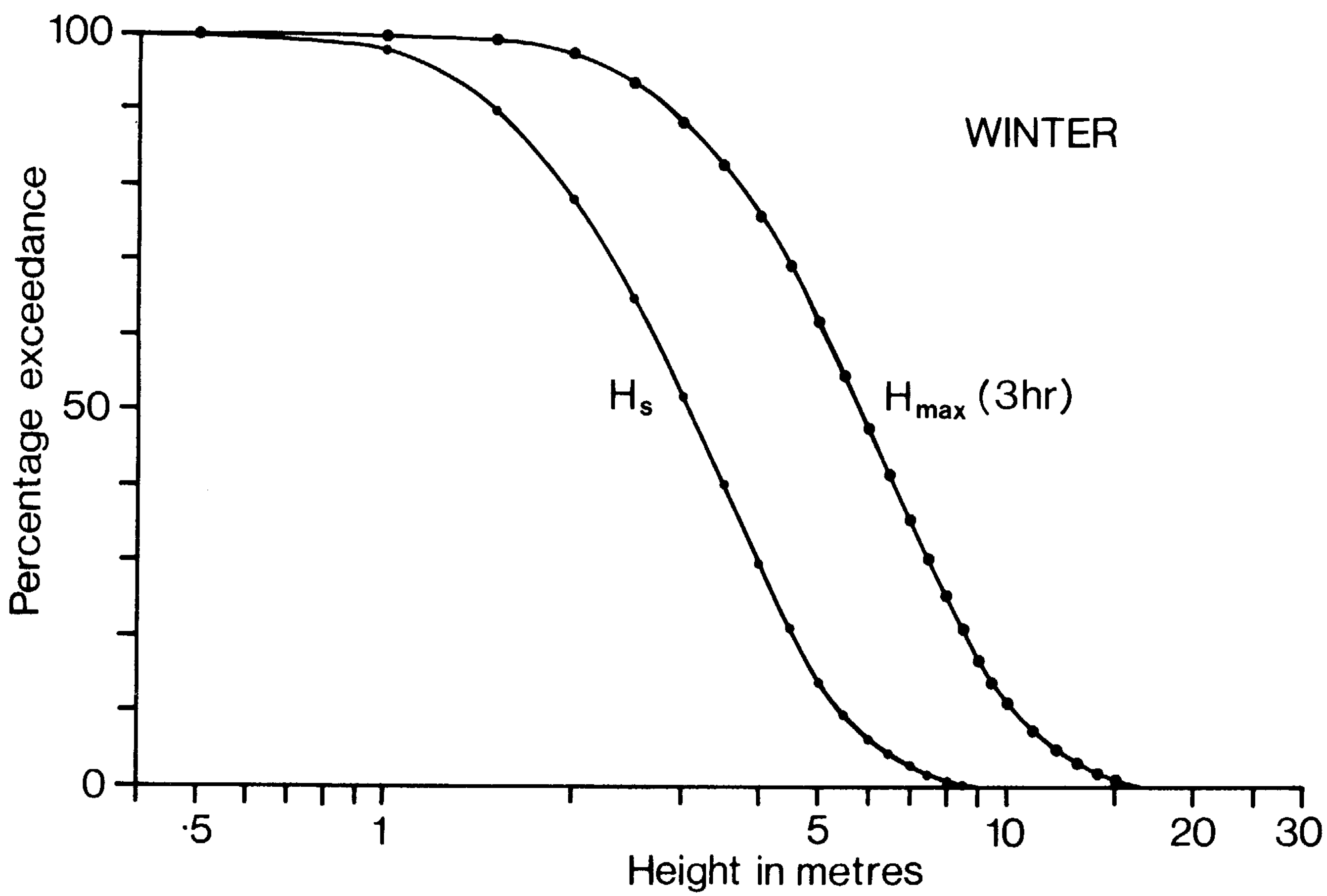

Percentage exceedance of H_s and H_{max} (3hr) - Winter

Fig. 4

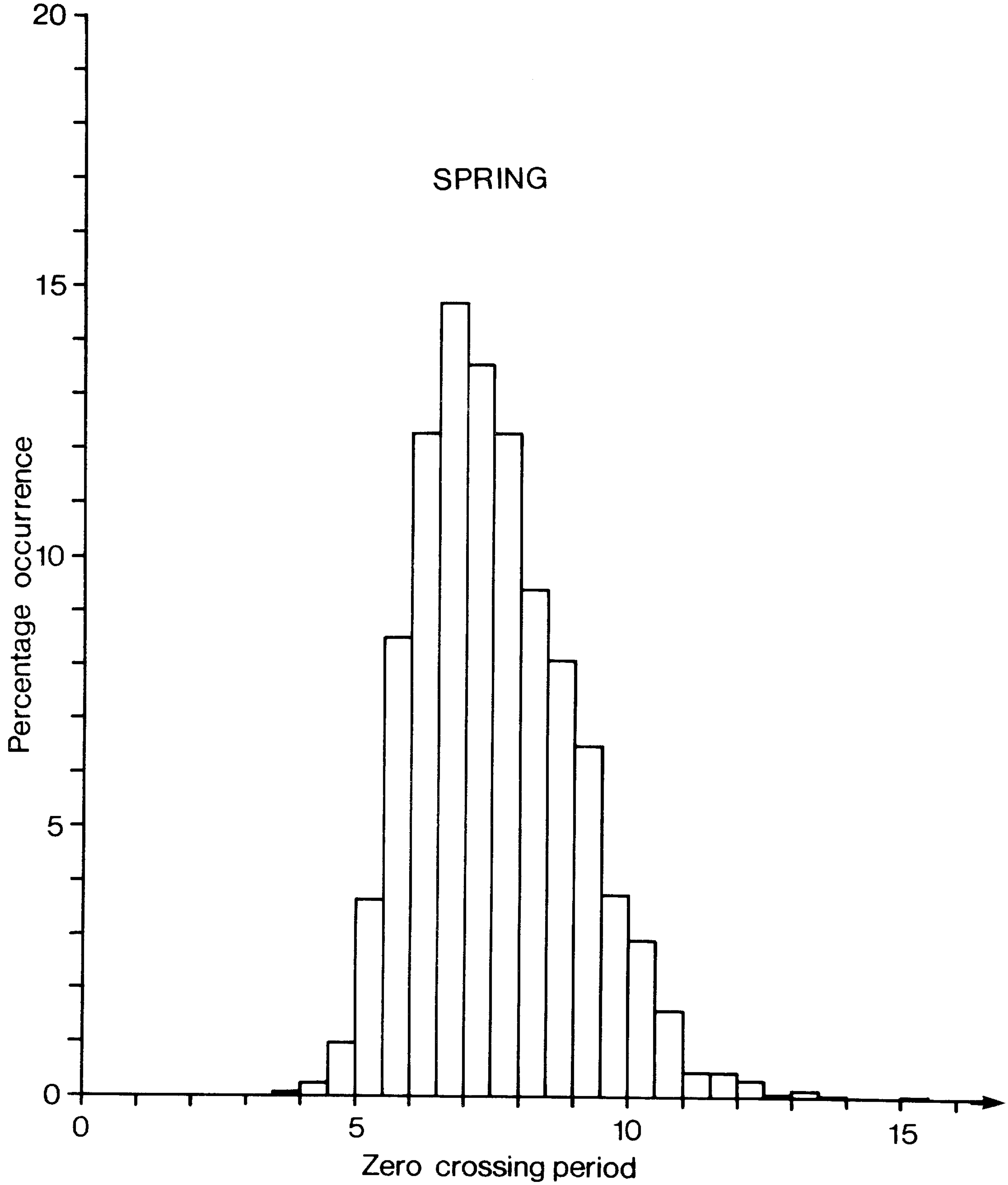

Frequency histogram for zero-crossing period - Spring.

Fig.5

SS

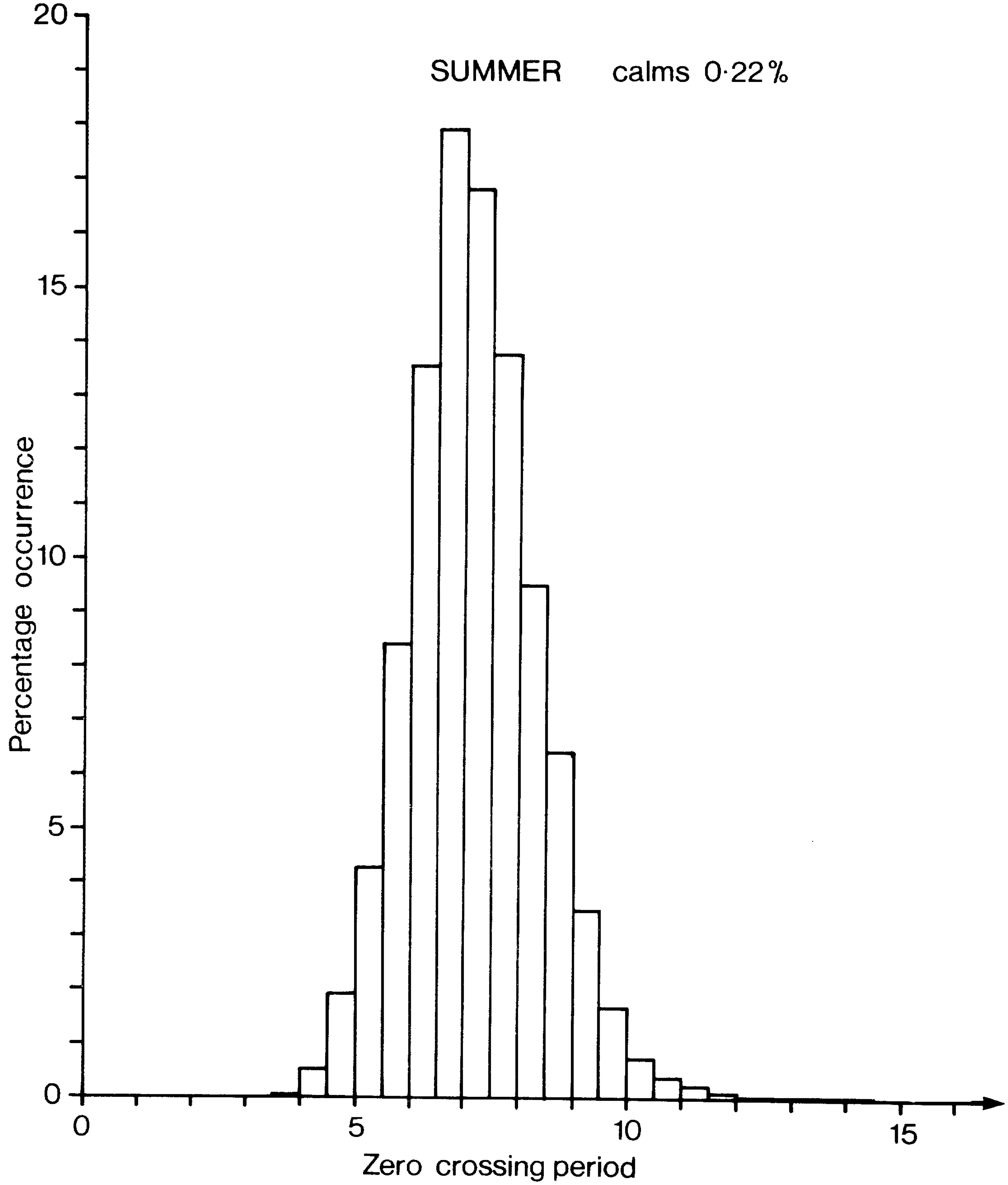

Frequency histogram for zero-crossing period - Summer.

Fig.6

SS

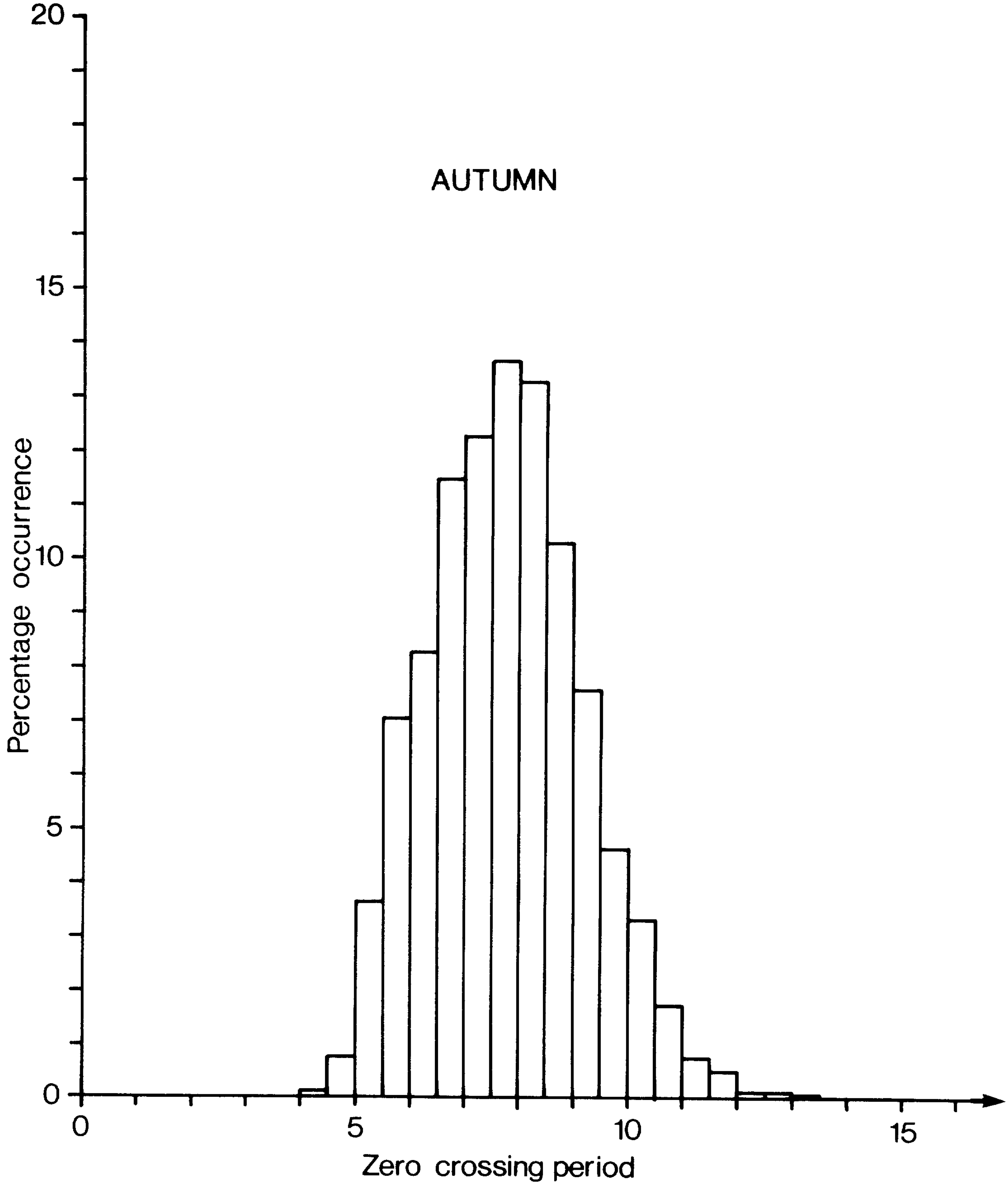

Frequency histogram for zero-crossing period - Autumn.

Fig. 7

SS

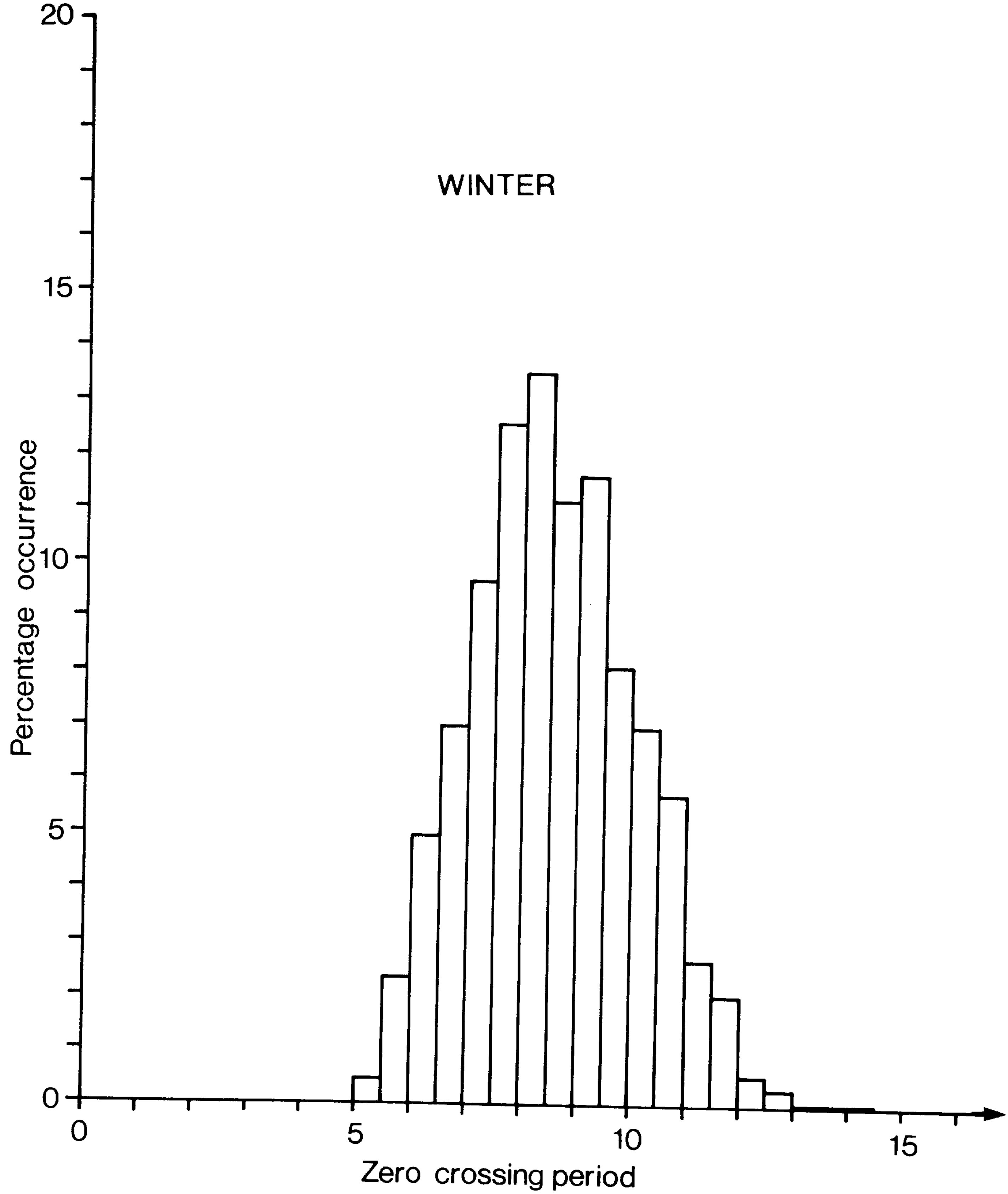

Frequency histogram for zero-crossing period - Winter.

Fig.8

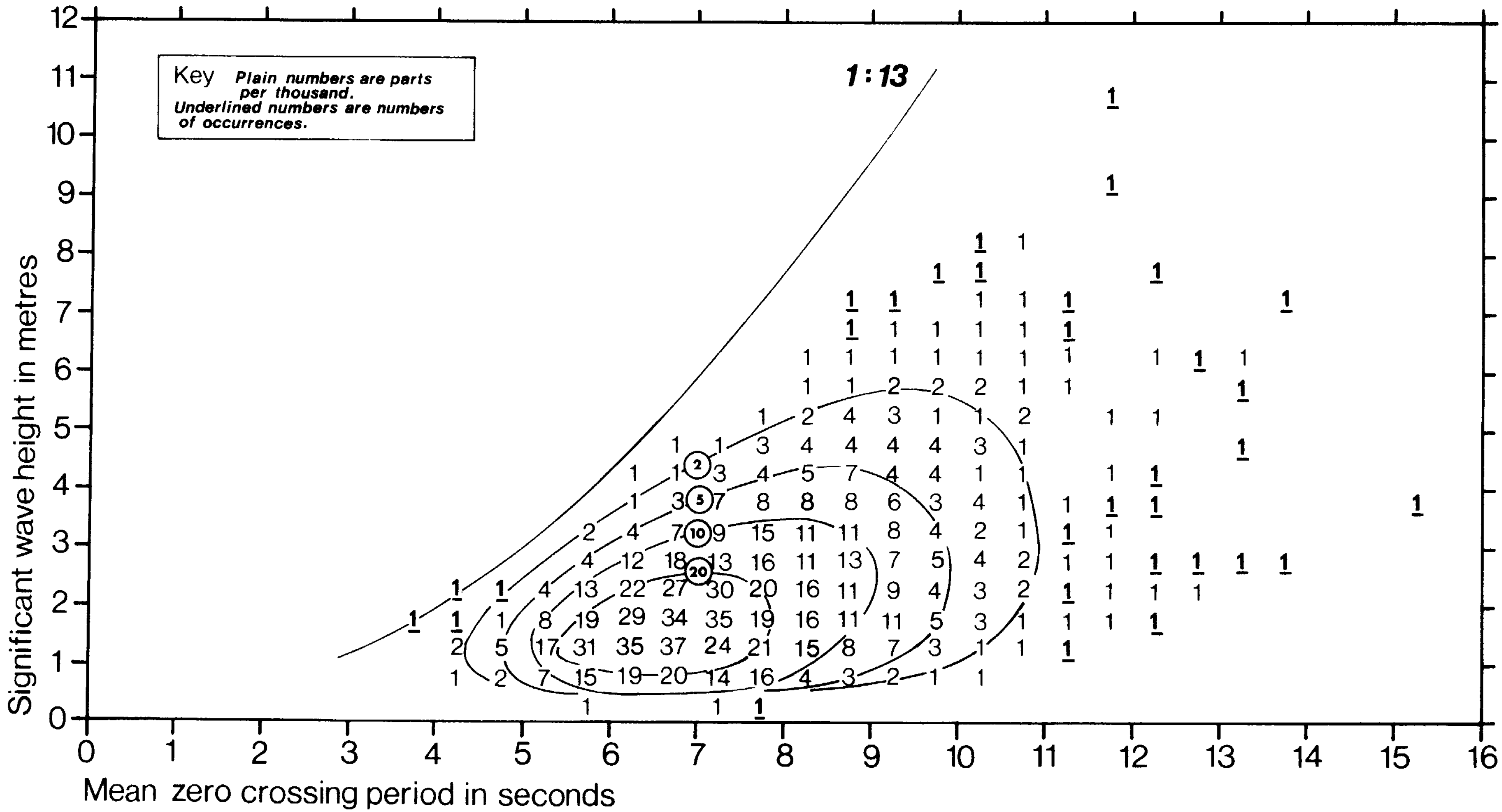

Scatter diagram in parts per thousand - Spring *March - May*

Fig. 9

SS

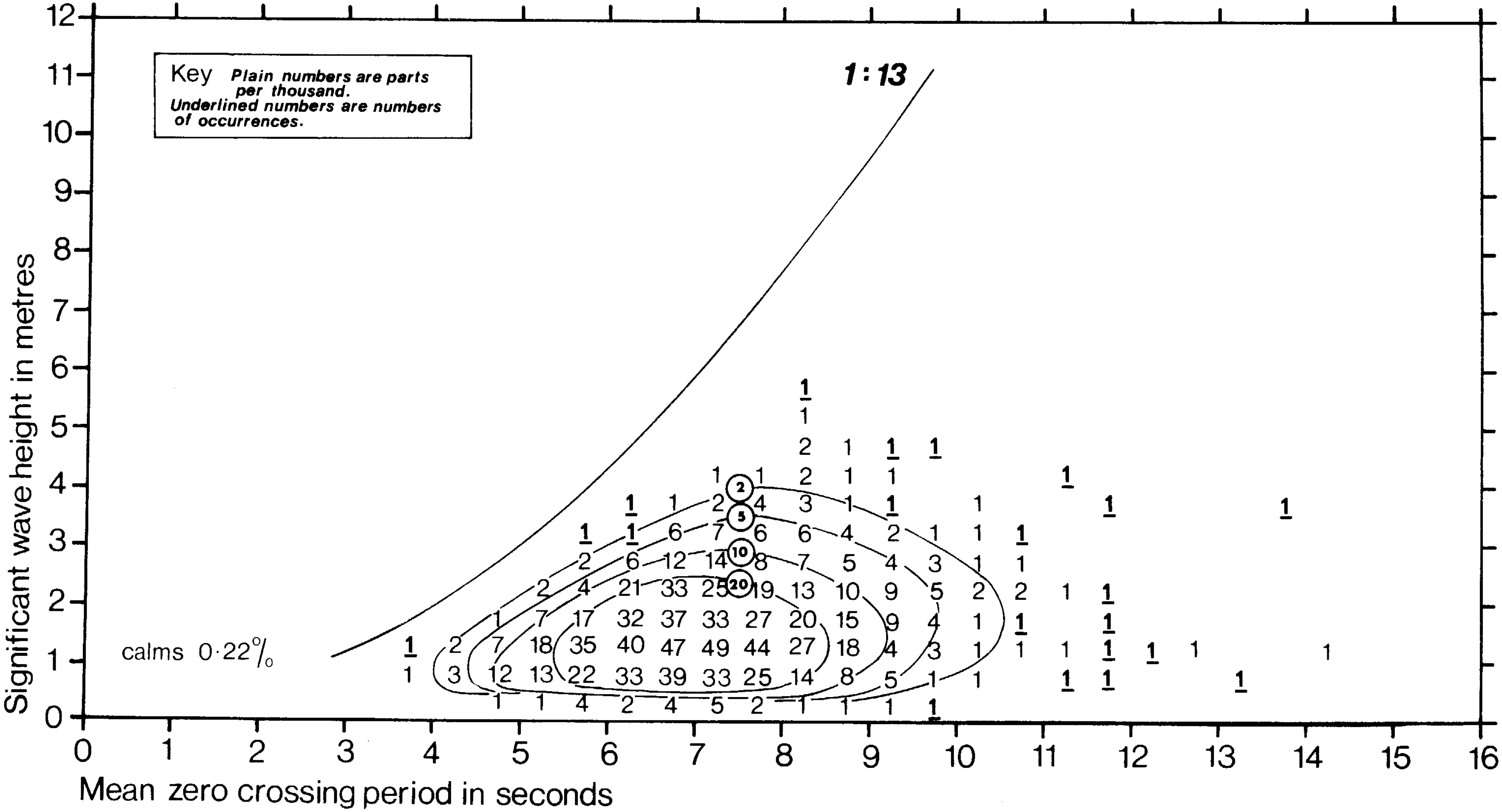

Scatter diagram in parts per thousand - Summer *Jun - Aug*

Fig.10

SS

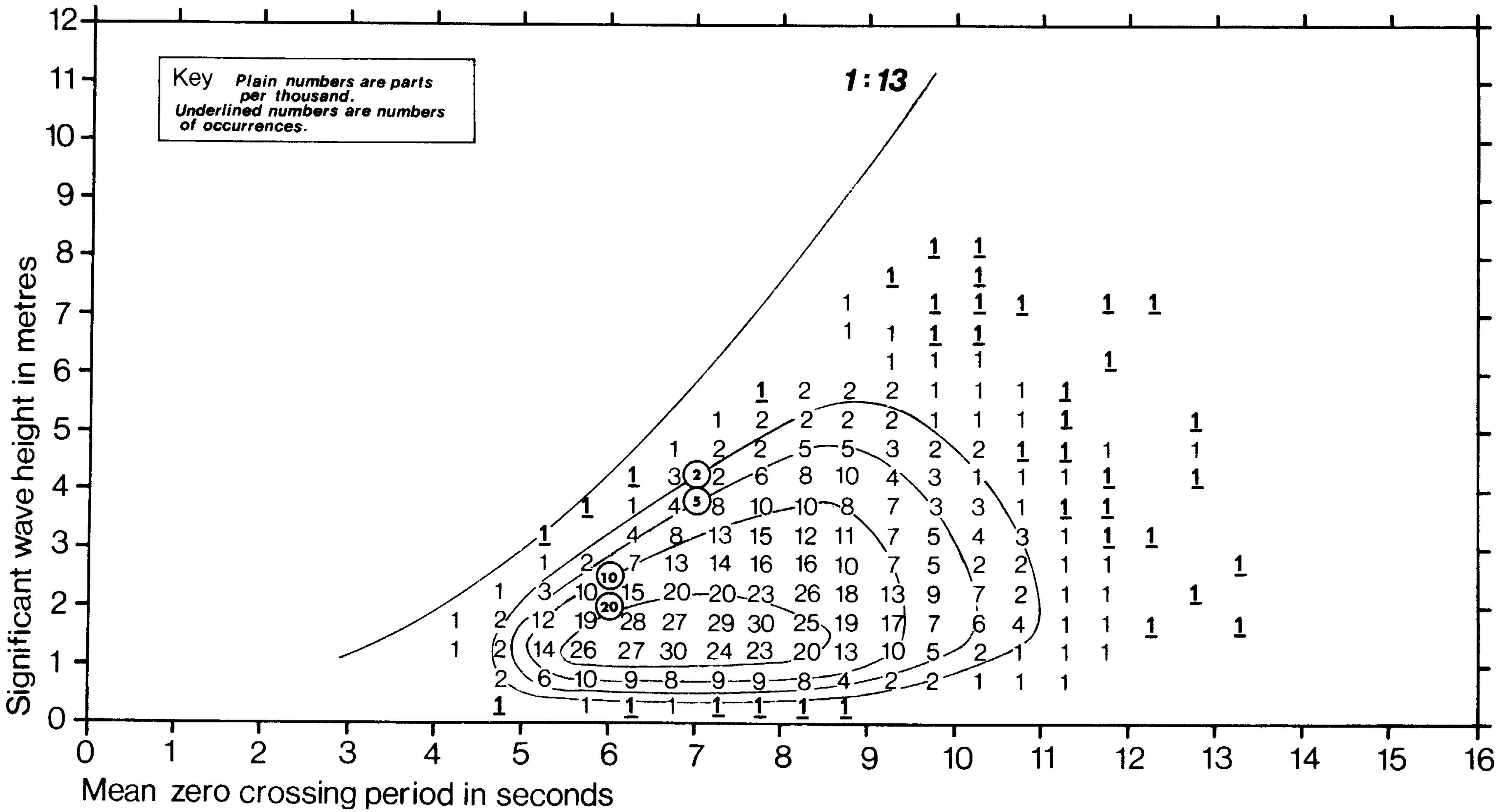

Scatter diagram in parts per thousand - Autumn *Sep - Nov*

Fig.11

SS

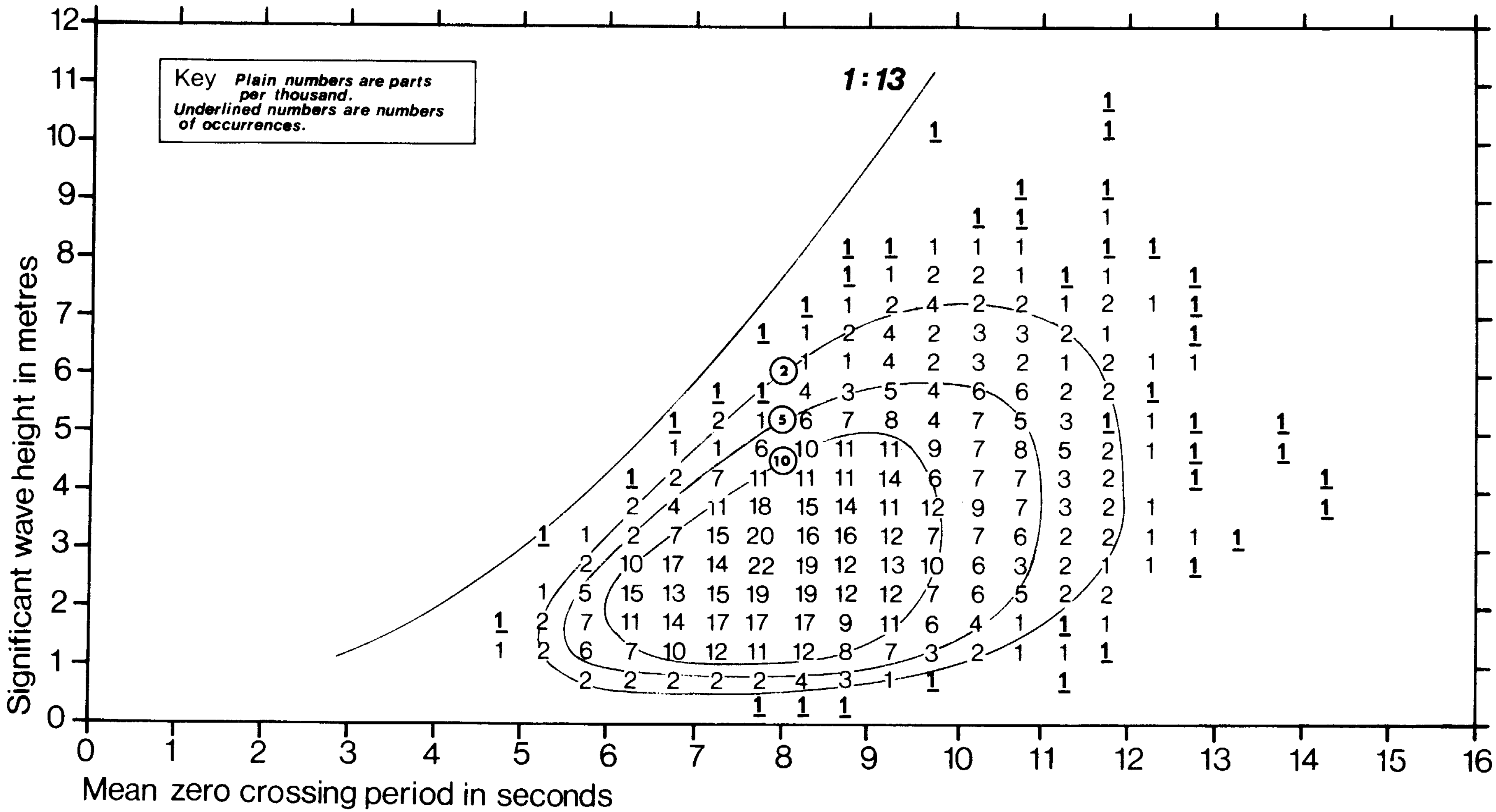

Scatter diagram in parts per thousand - Winter *Dec - Feb*

Fig. 12

SS

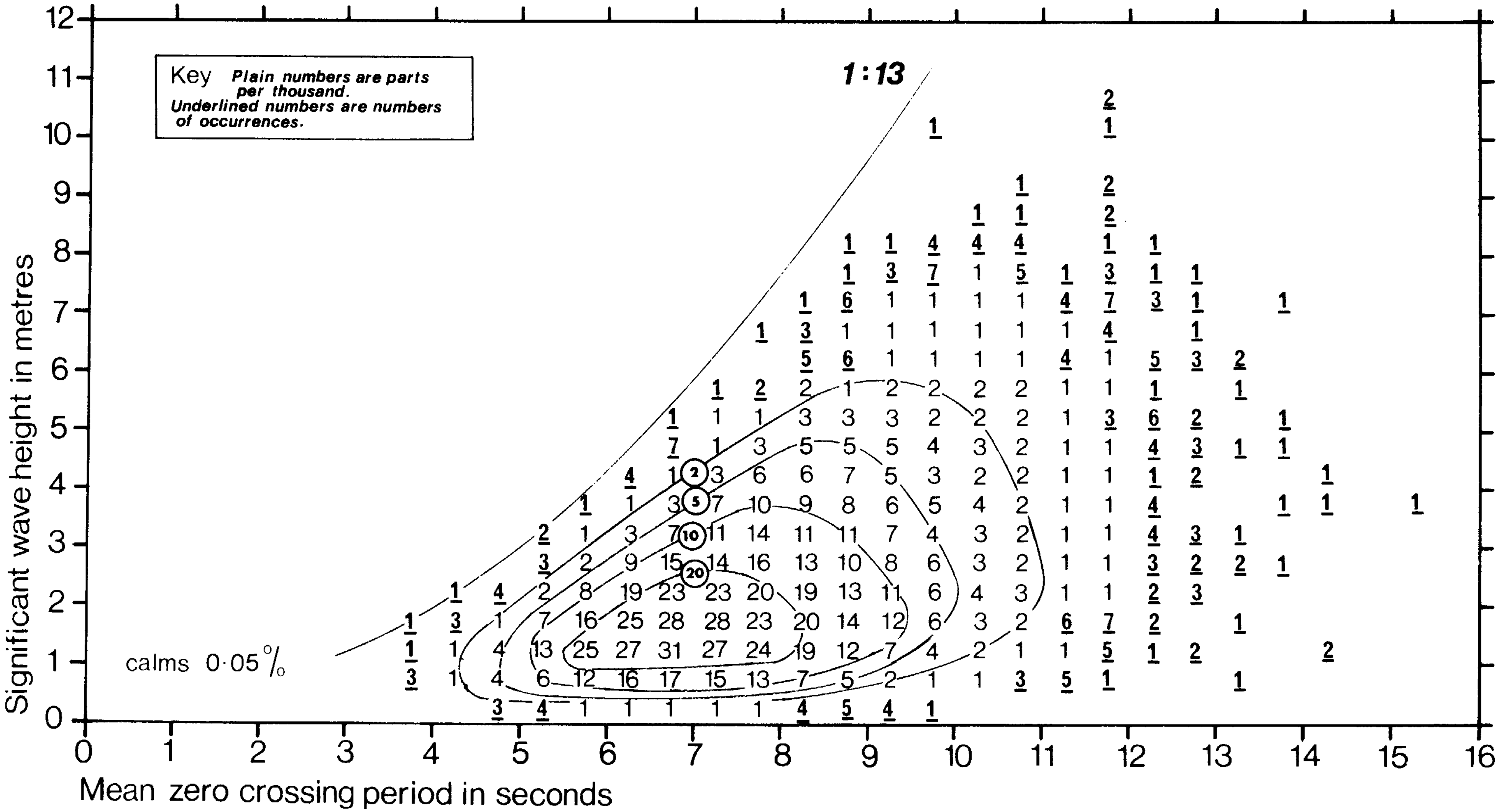

Scatter diagram in parts per thousand - Whole year

Fig. 13

SS

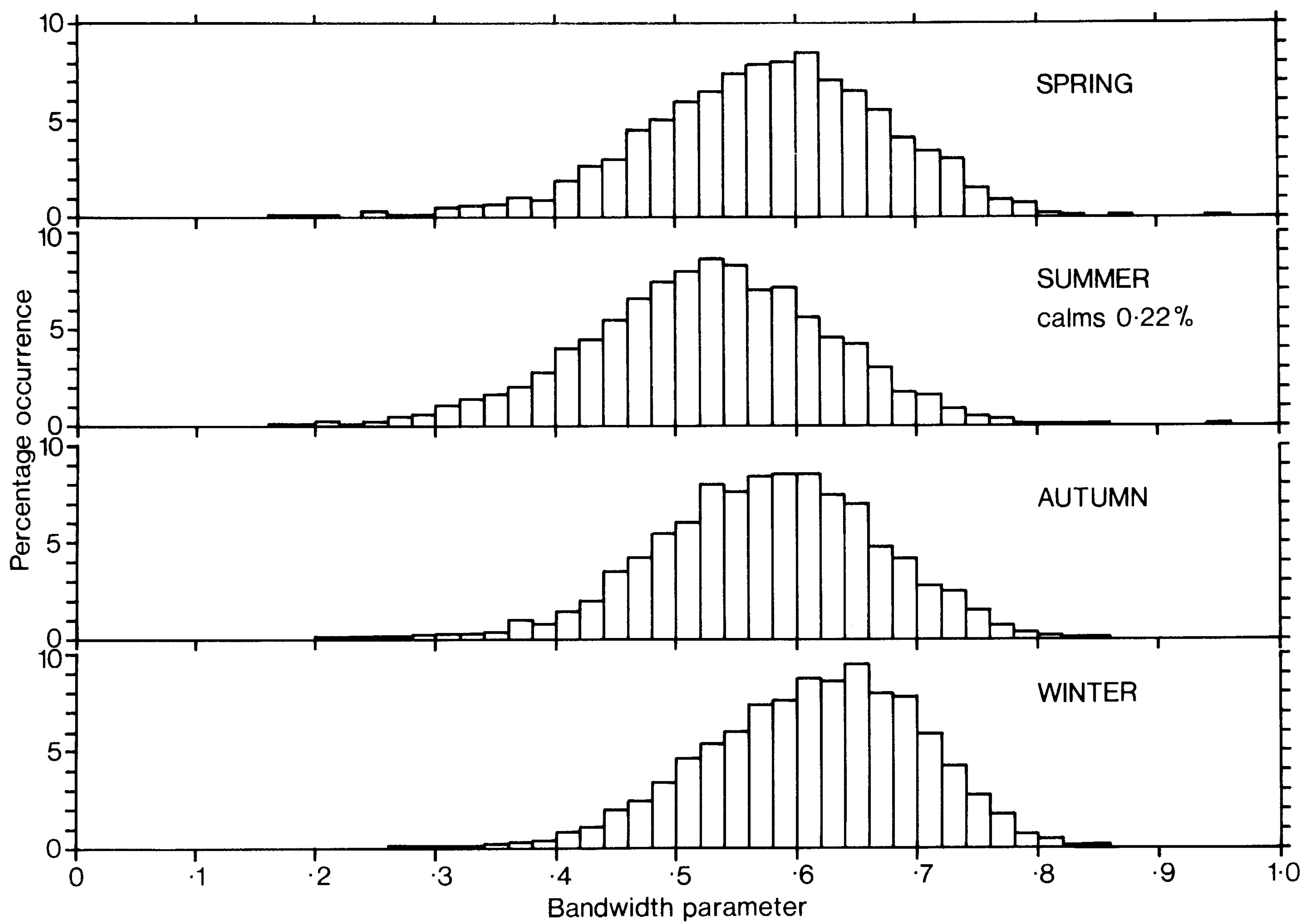

Frequency histograms for Bandwidth parameter.
Fig.14

SS

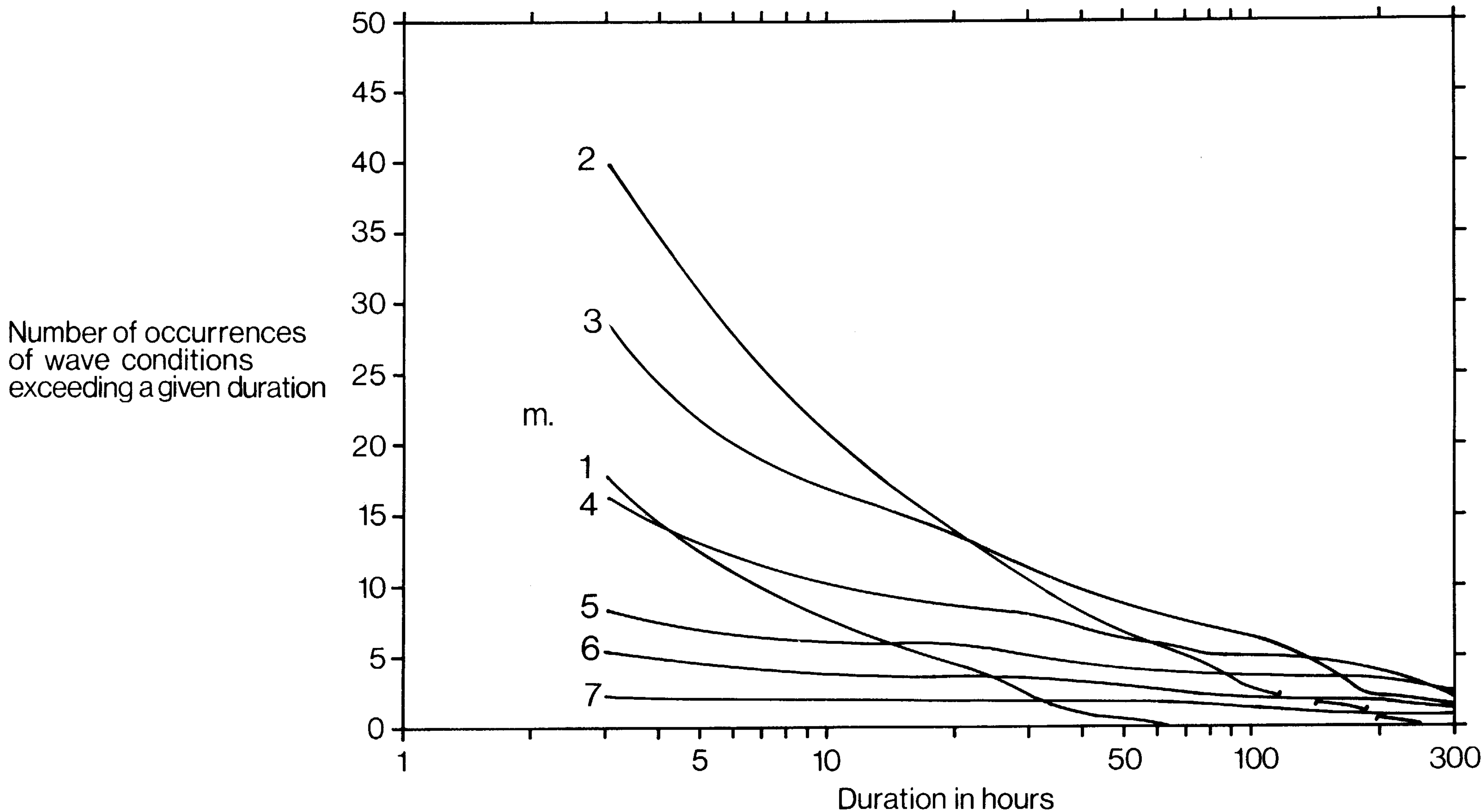

Persistence of Calms - Spring

Fig. 15

SS

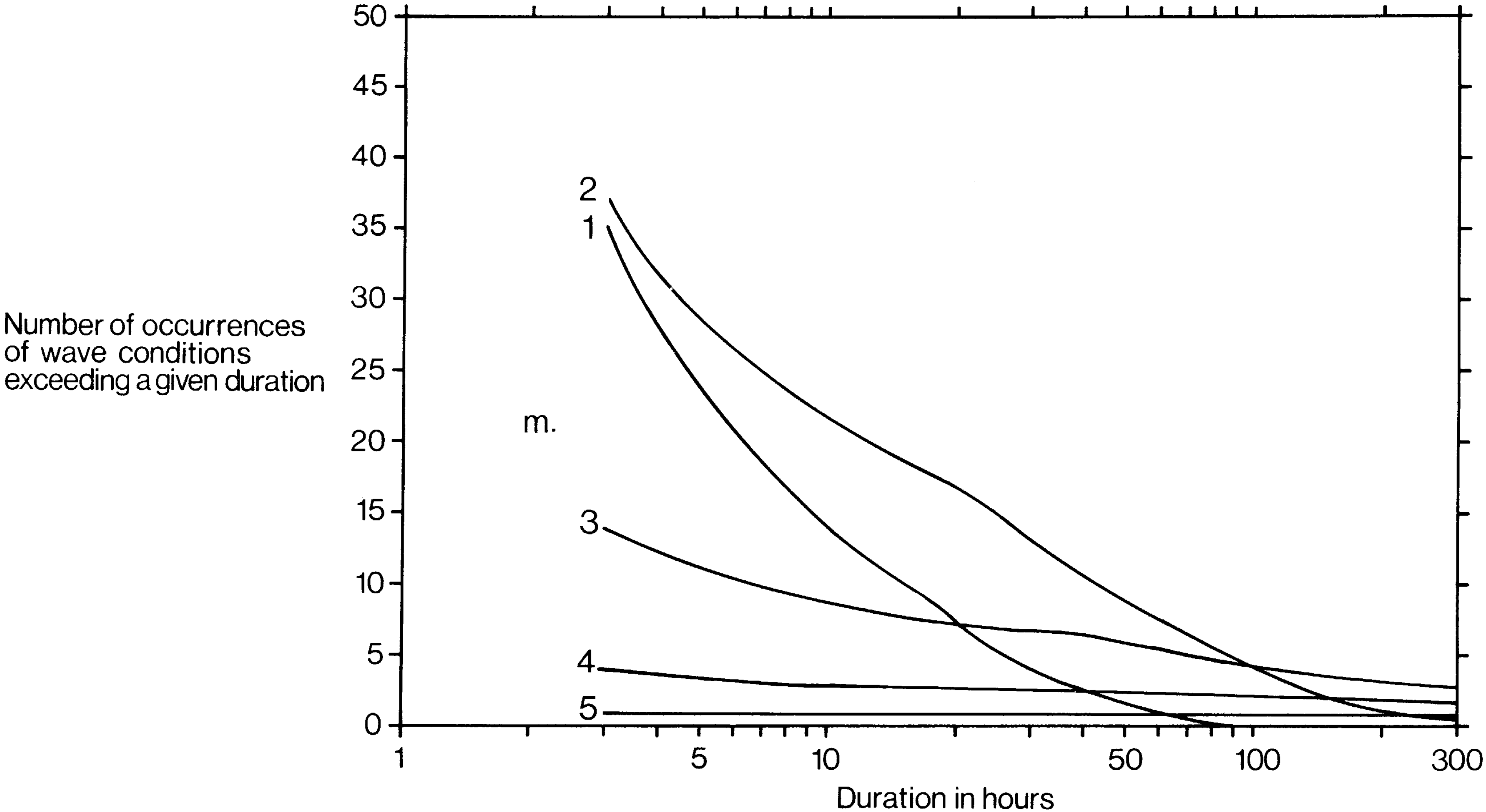

Persistence of Calms - Summer

Fig.16

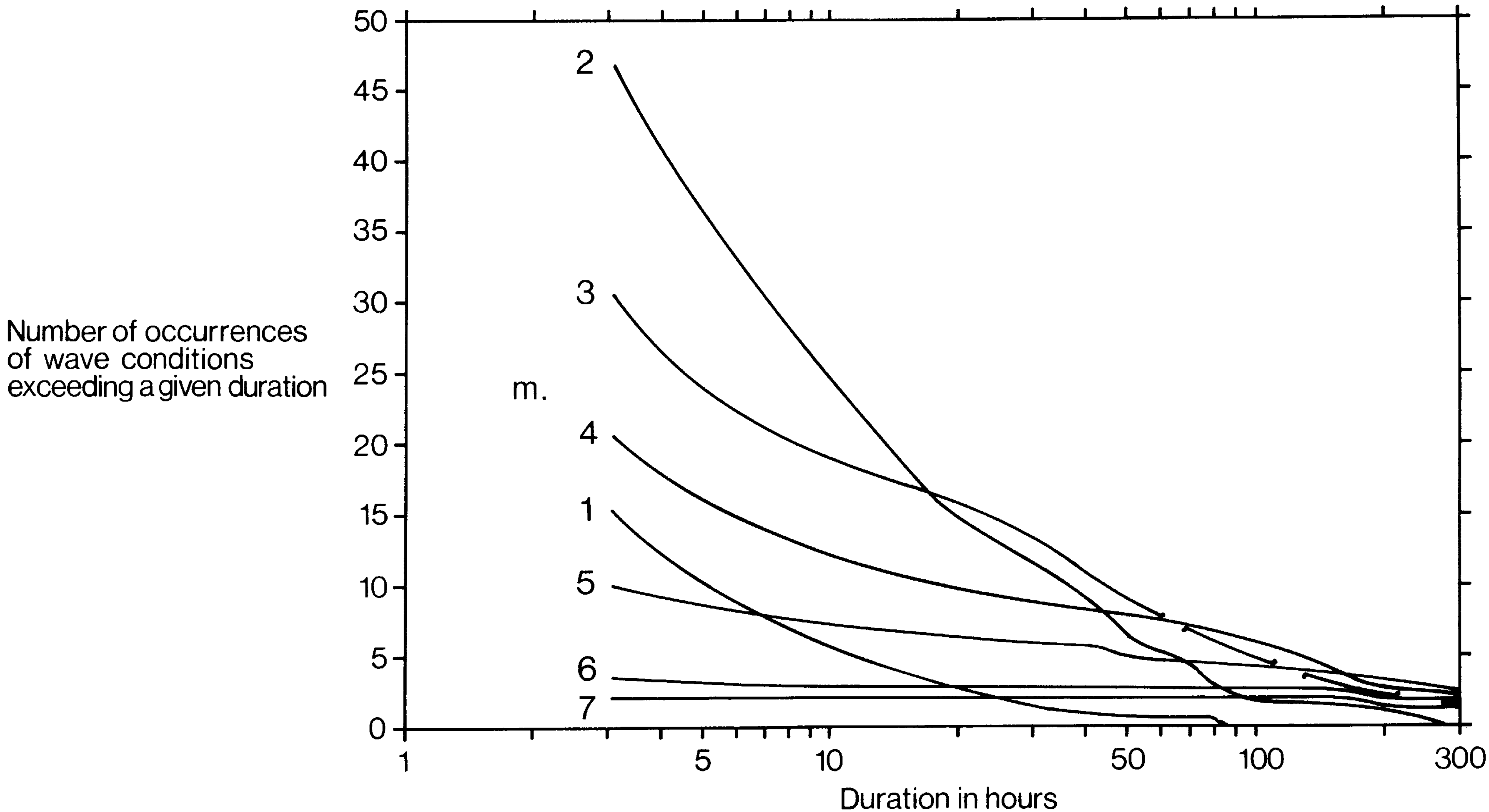

Persistence of Calms - Autumn

Fig.17

SS

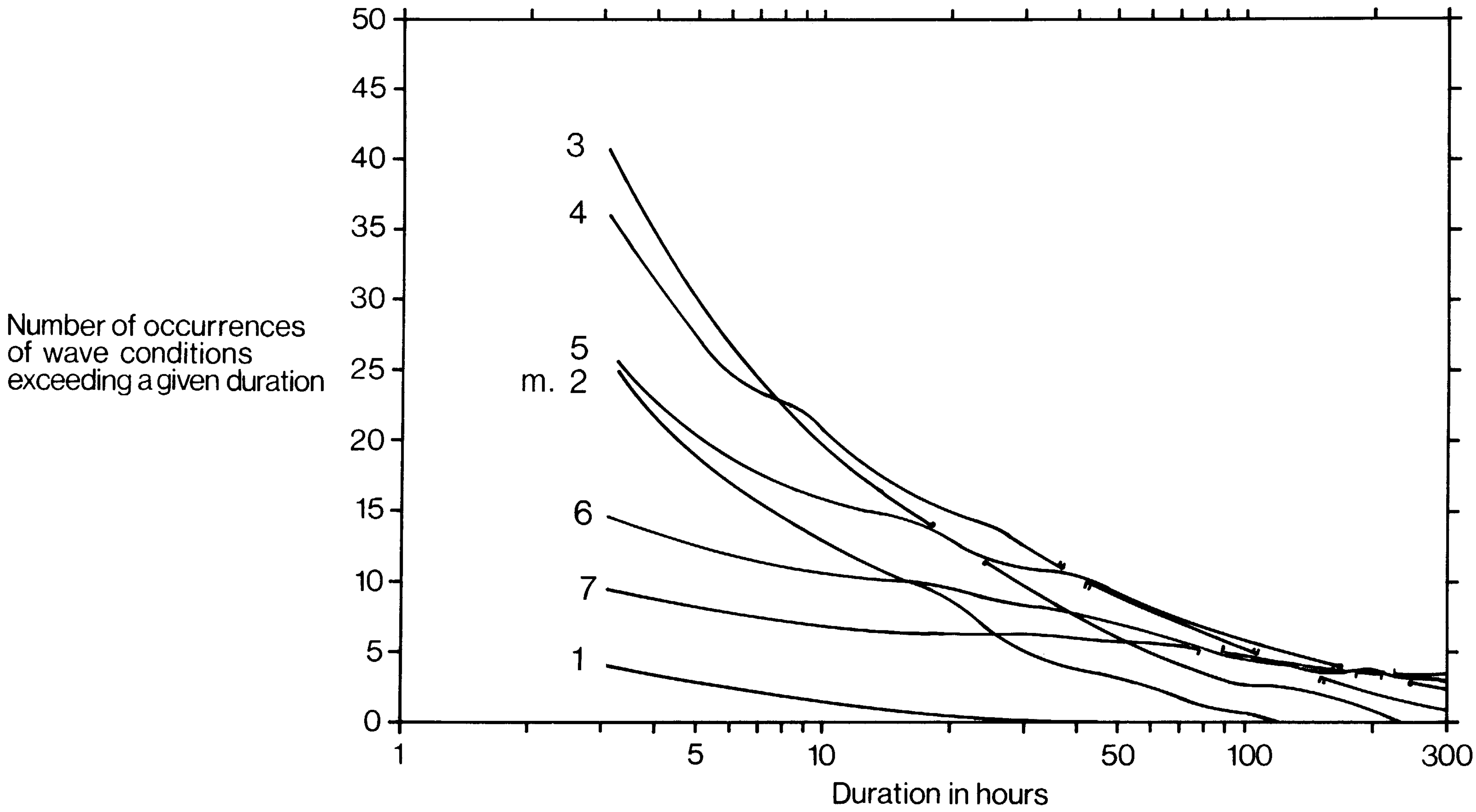

Persistence of Calms - Winter

Fig. 18

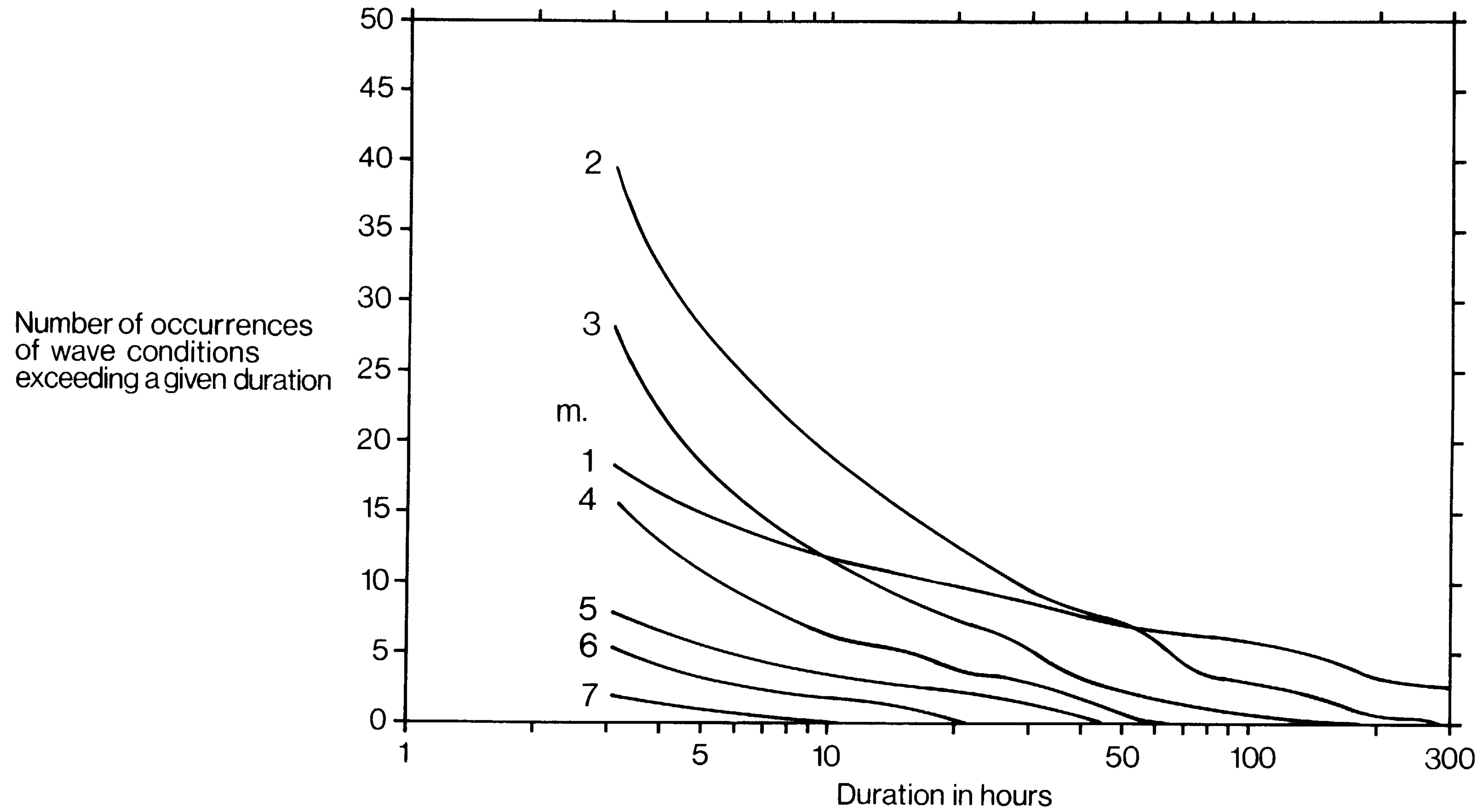

Persistence of Storms - Spring

Fig. 19

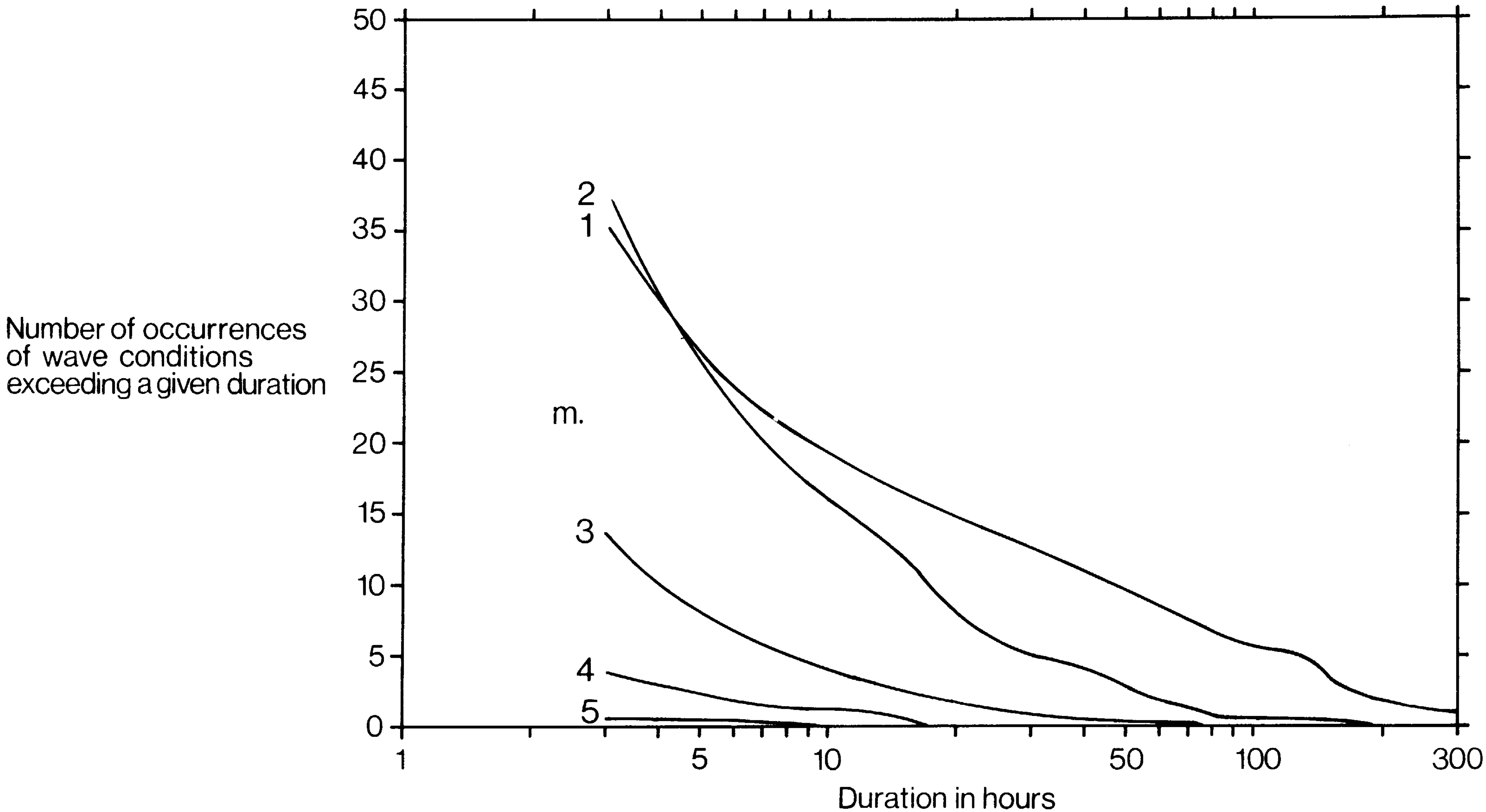

Persistence of Storms - Summer

Fig. 20

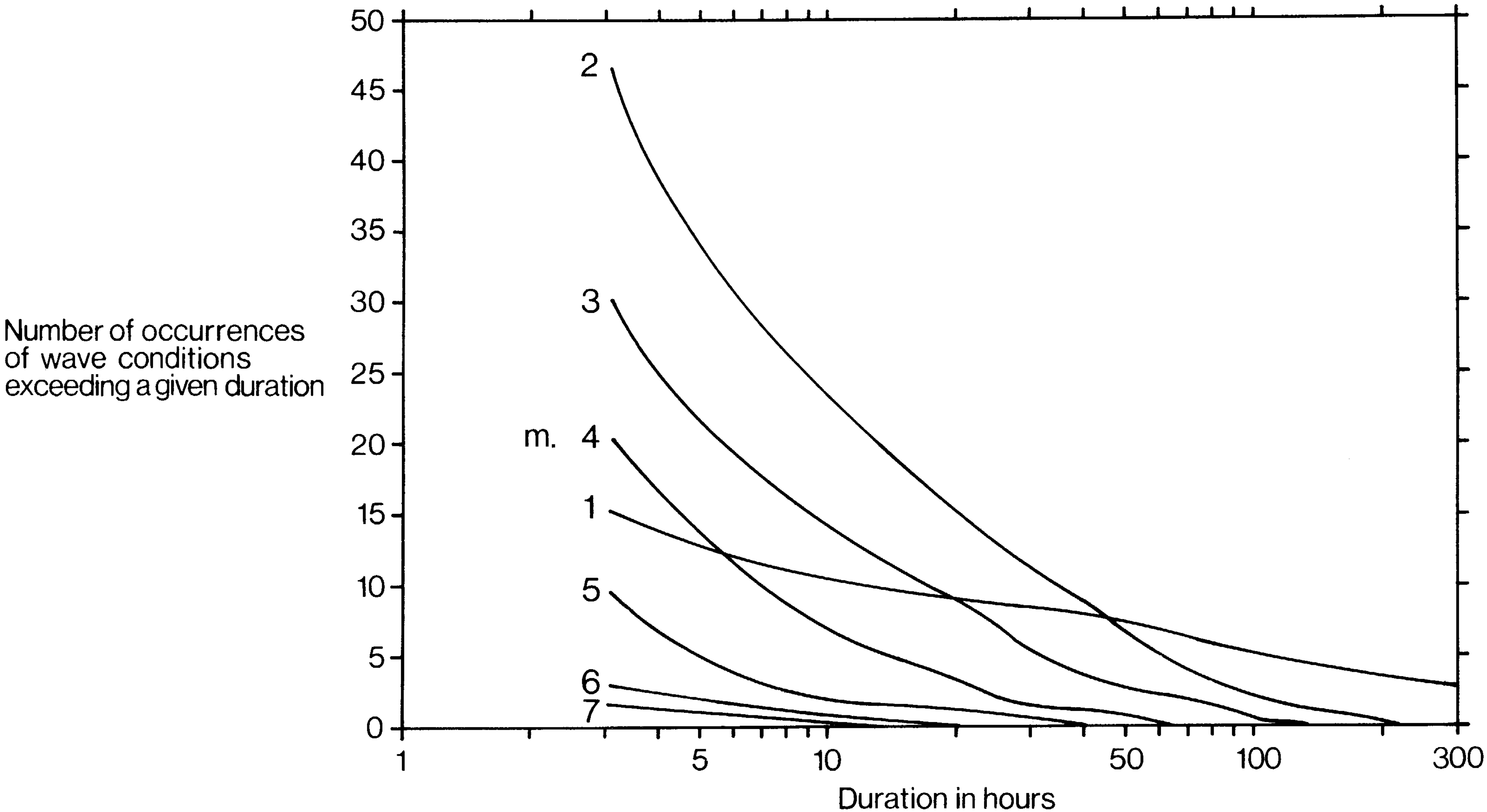

Persistence of Storms – Autumn
Fig. 21

SS

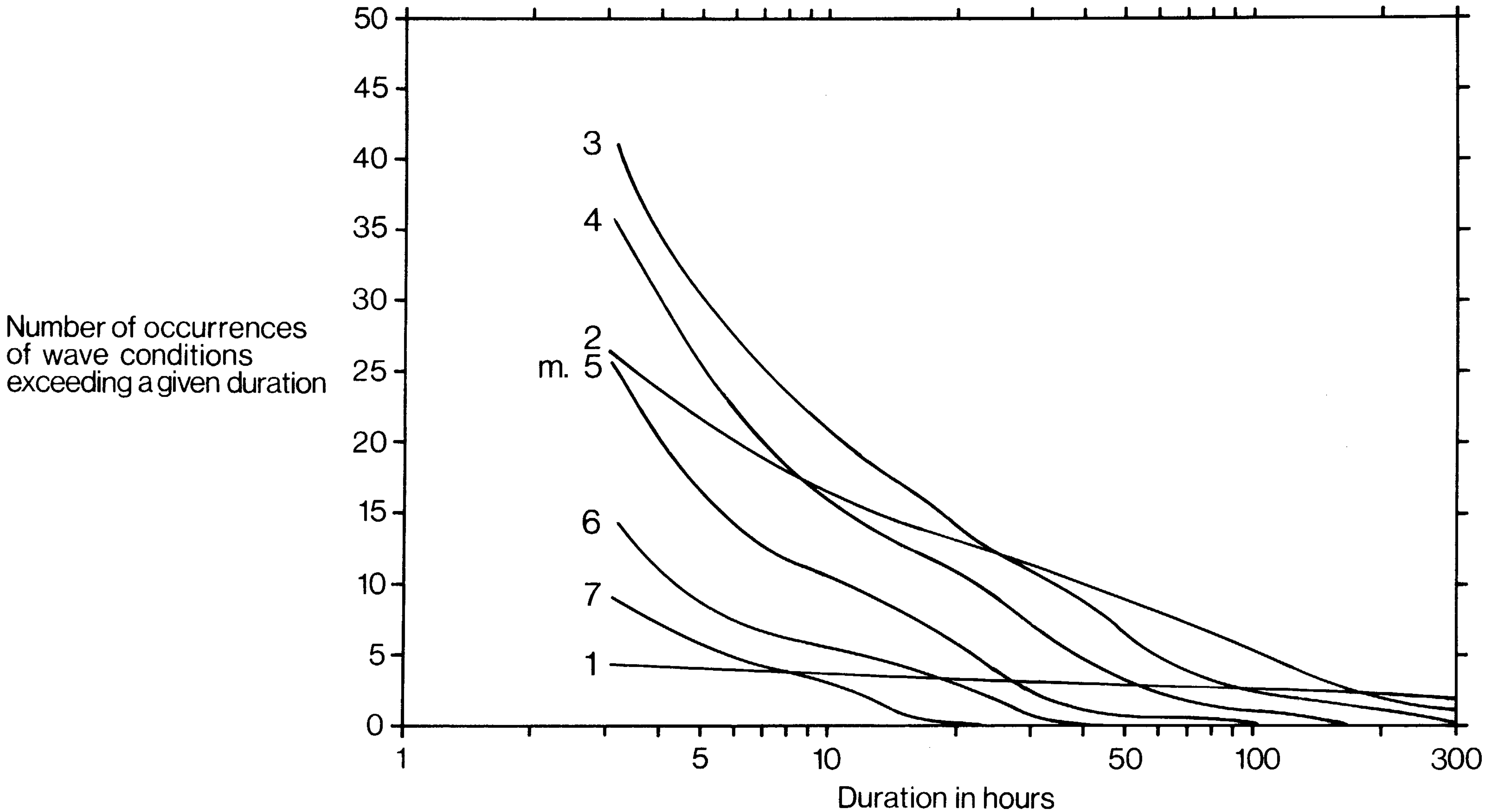

Persistence of Storms - Winter

Fig.22

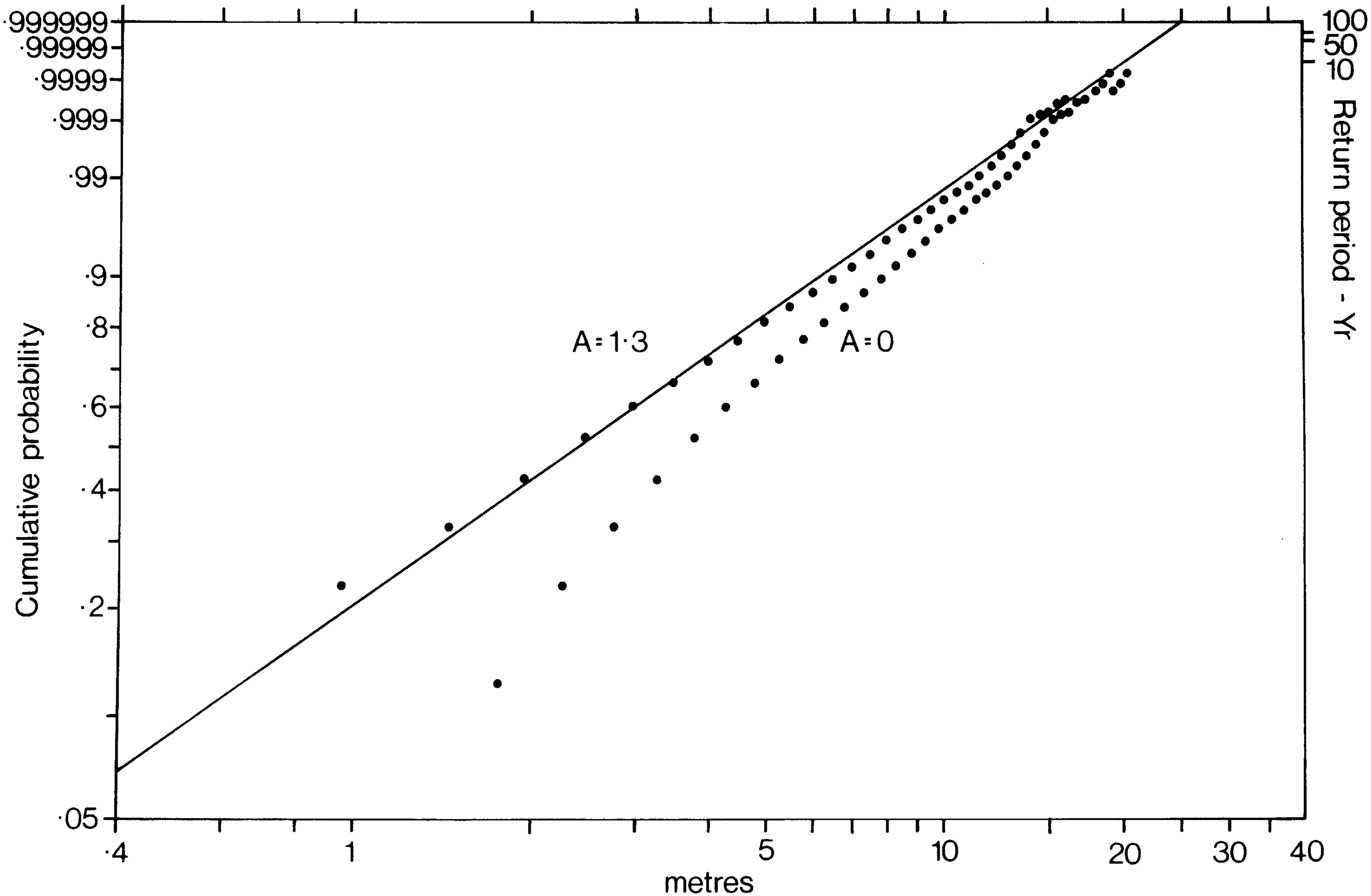

Cumulative distribution of H_{max} (3hr) Weibull scale

Fig.23

SS

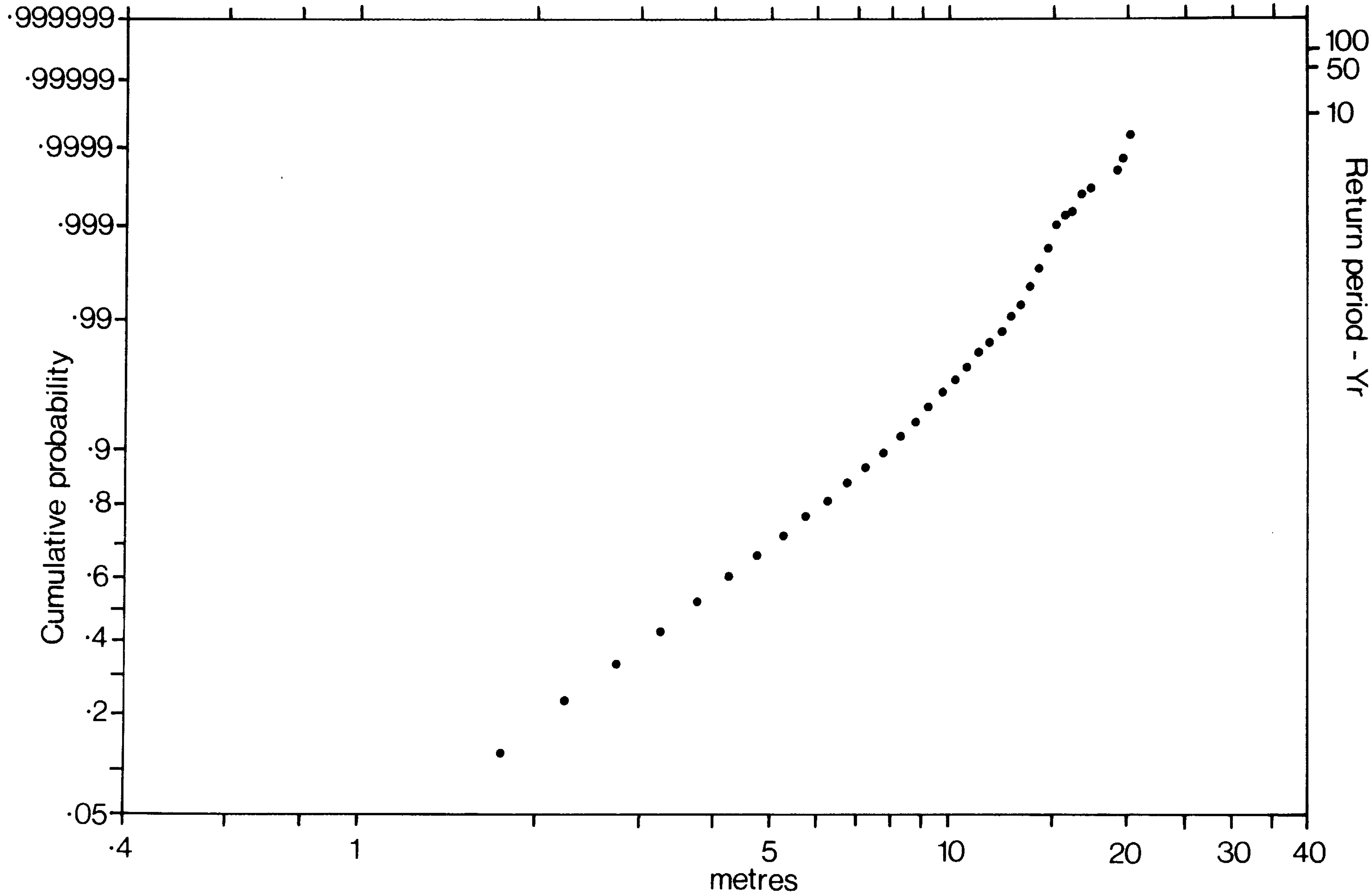

Cumulative distribution of H_{max} (3hr) Log normal scale
Fig. 24

SS

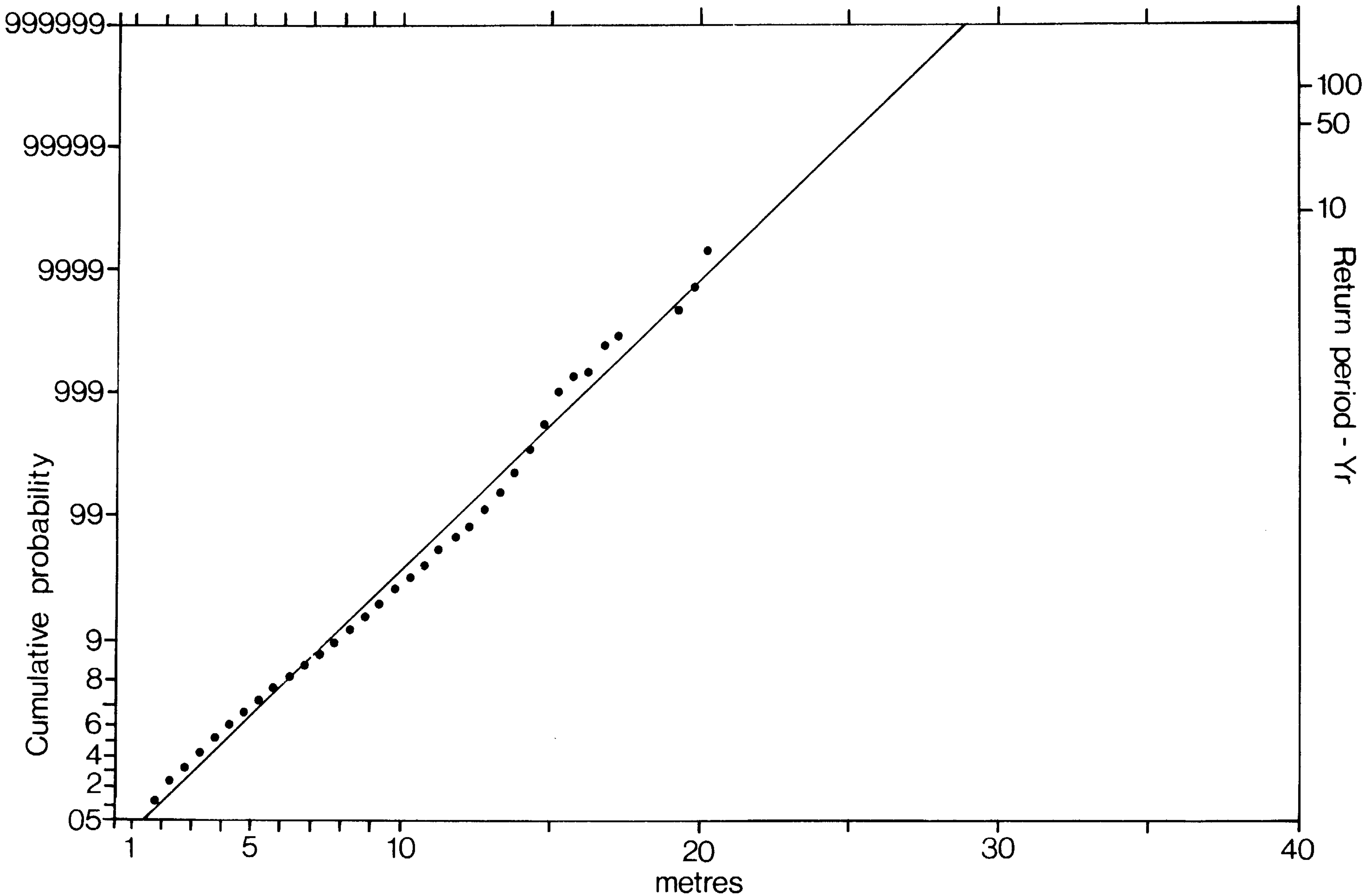

Cumulative distribution of H_{max} (3hr) Gumbel I scale

Fig. 25

SS

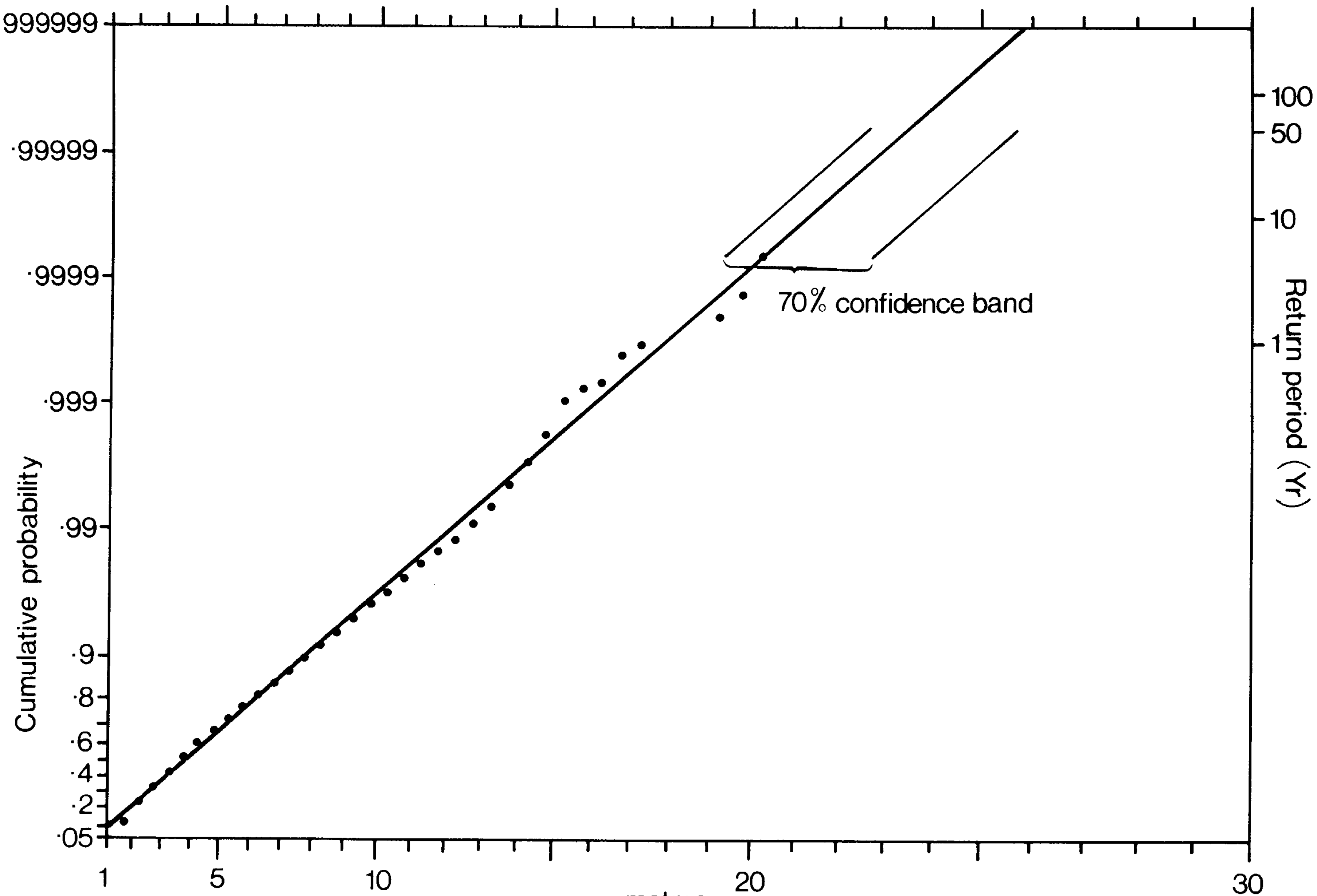

Cumulative distribution of H_{max} (3hr) Gumbel III scale (A=55m)

Fig.26

SS

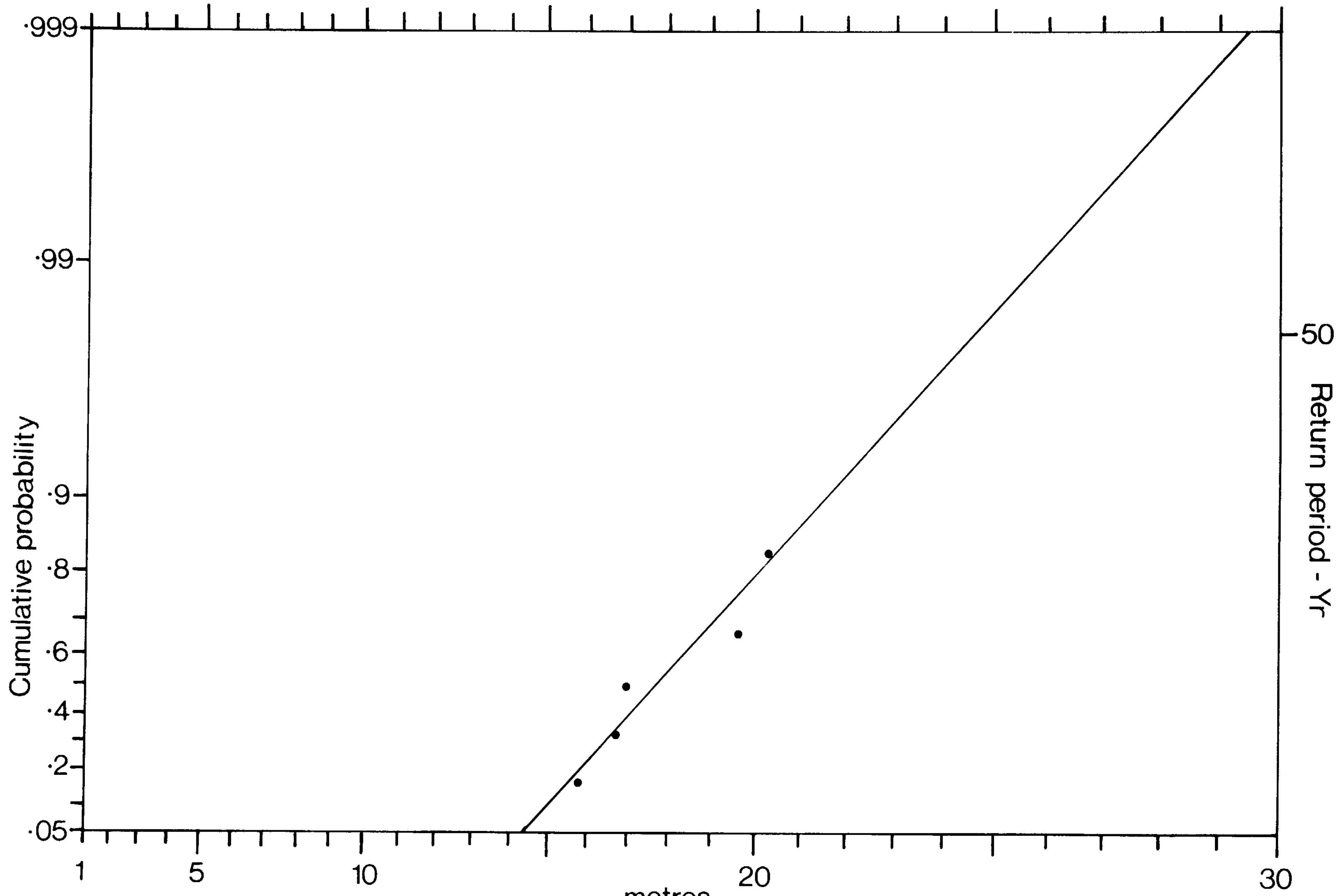

Cumulative distribution of yearly maxima of H_{max} (3hr) Gumbel III scale (A=55m)

Fig. 27

SS

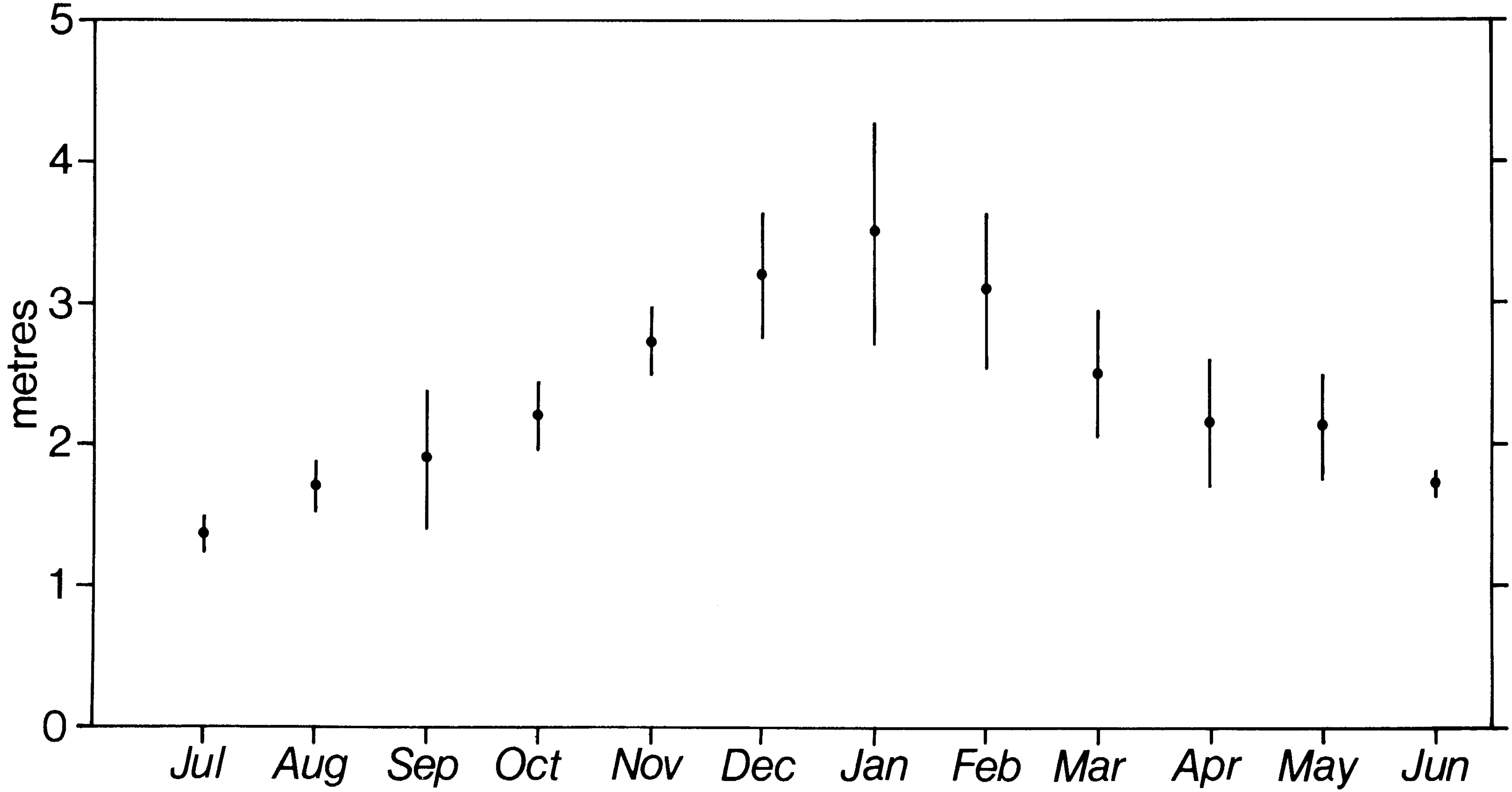

The mean and standard deviation of the average value of significant wave height for each month.

Fig.28

SS

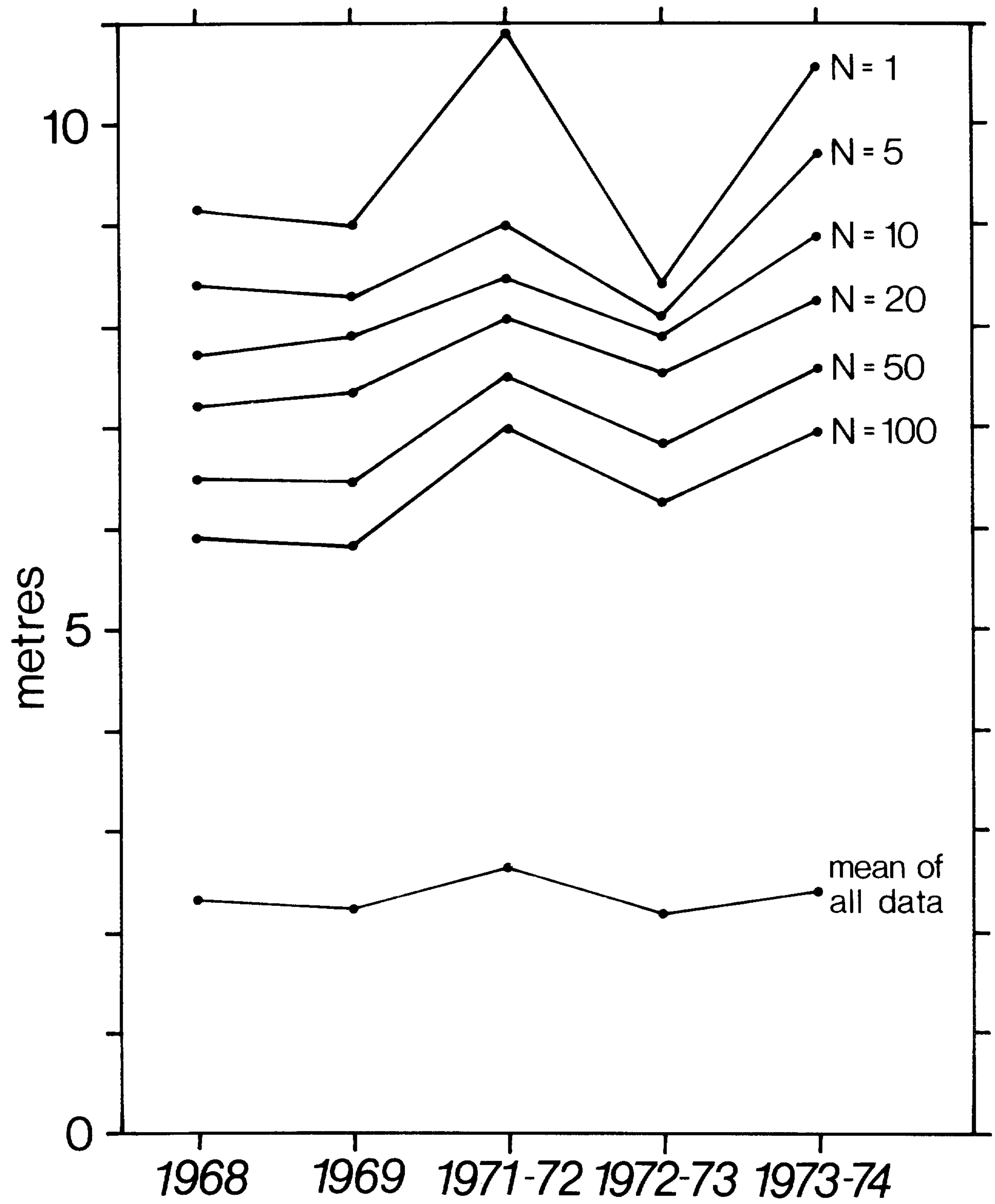

Mean of largest 'N' values of significant wave height.

Fig. 29

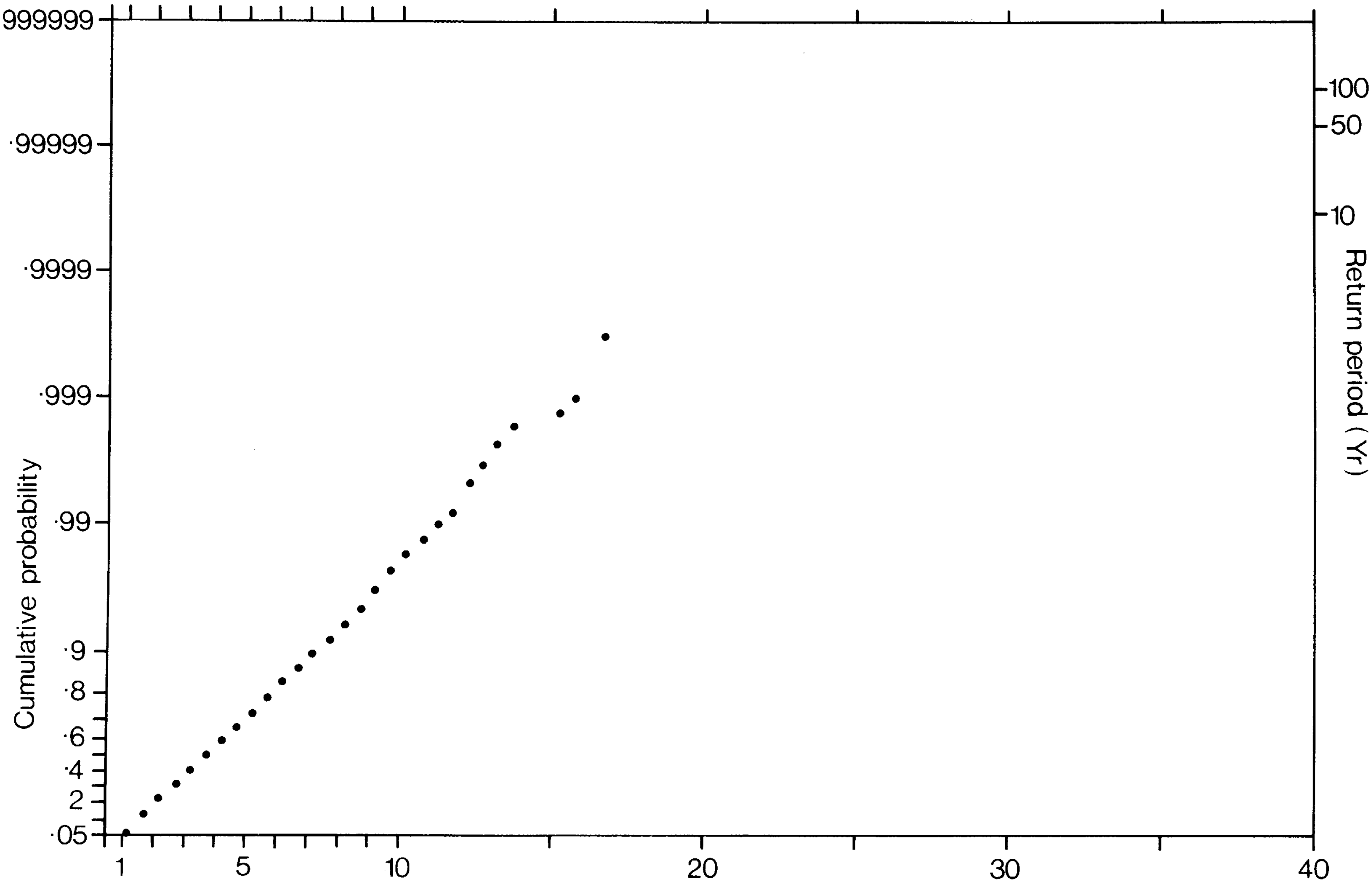

Cumulative distribution of H_{max} (3hr) Gumbel I scale *Jan 68 - Dec 68*

Fig. 30

SS

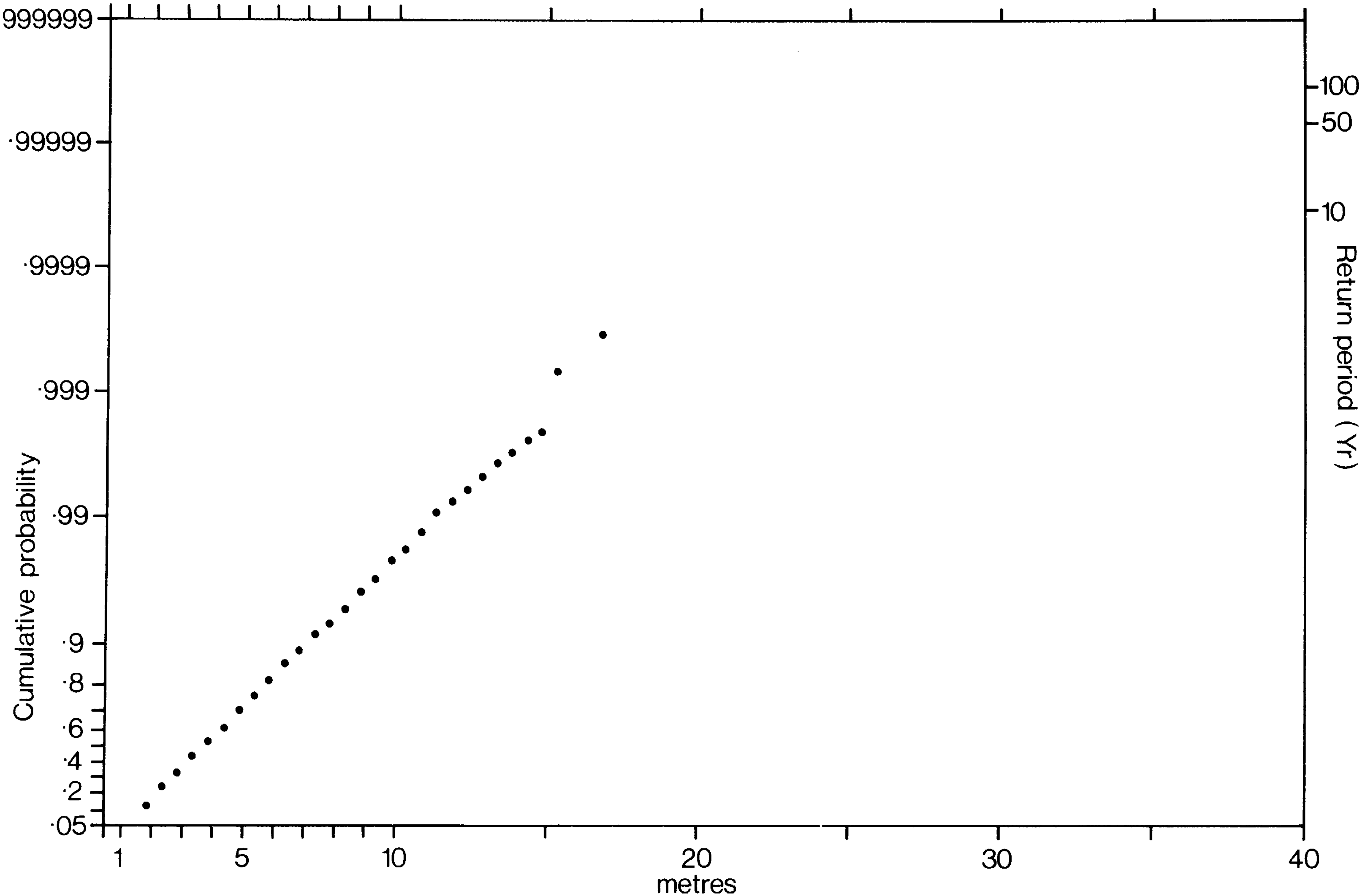

Cumulative distribution of H_{max} (3hr) Gumbel I scale *Jan 69 - Dec 69*

Fig. 31

SS

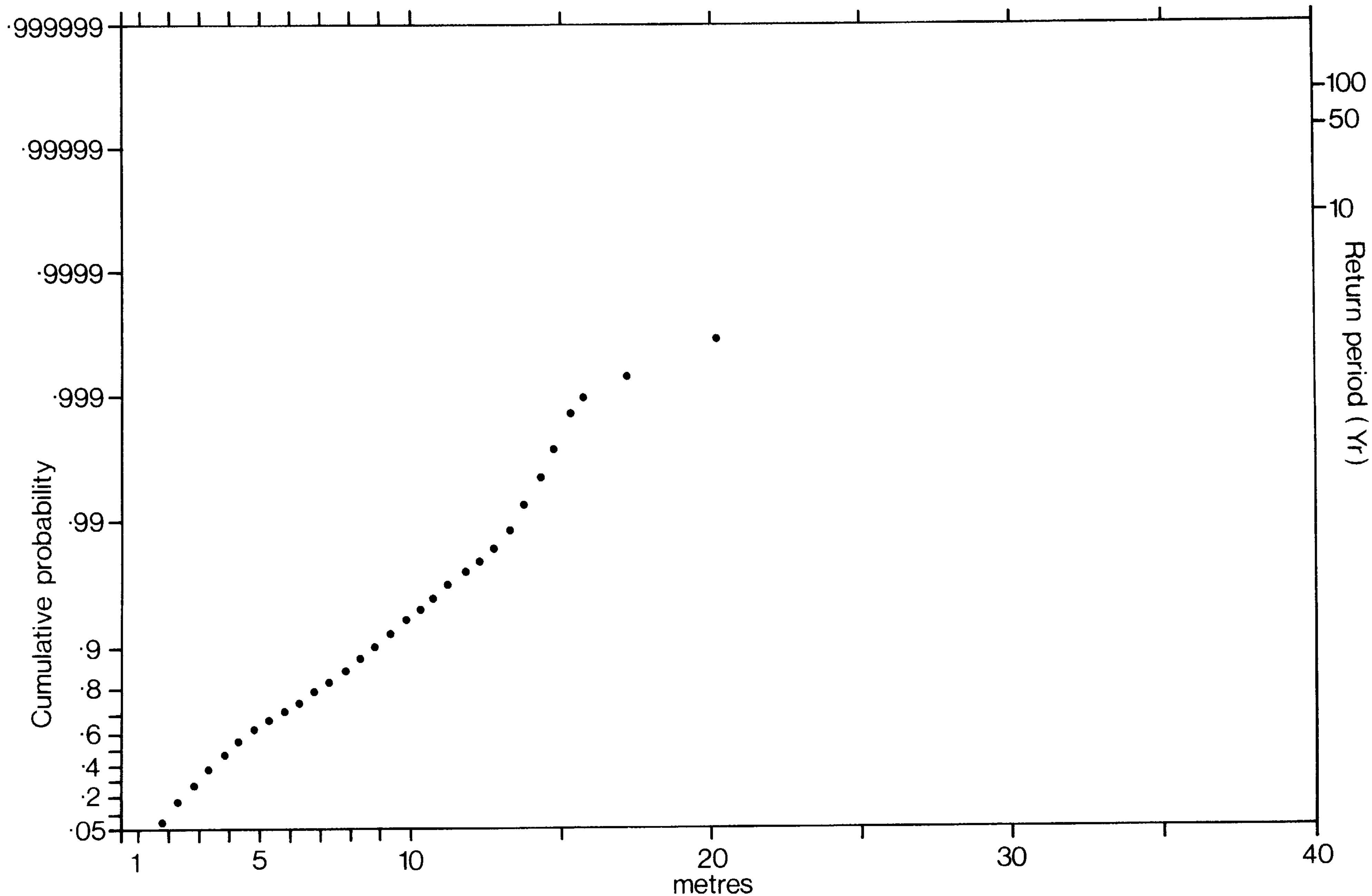

Cumulative distribution of H_{max} (3hr) Gumbel I scale ***Jul 71 - Jun 72***

Fig. 32

SS

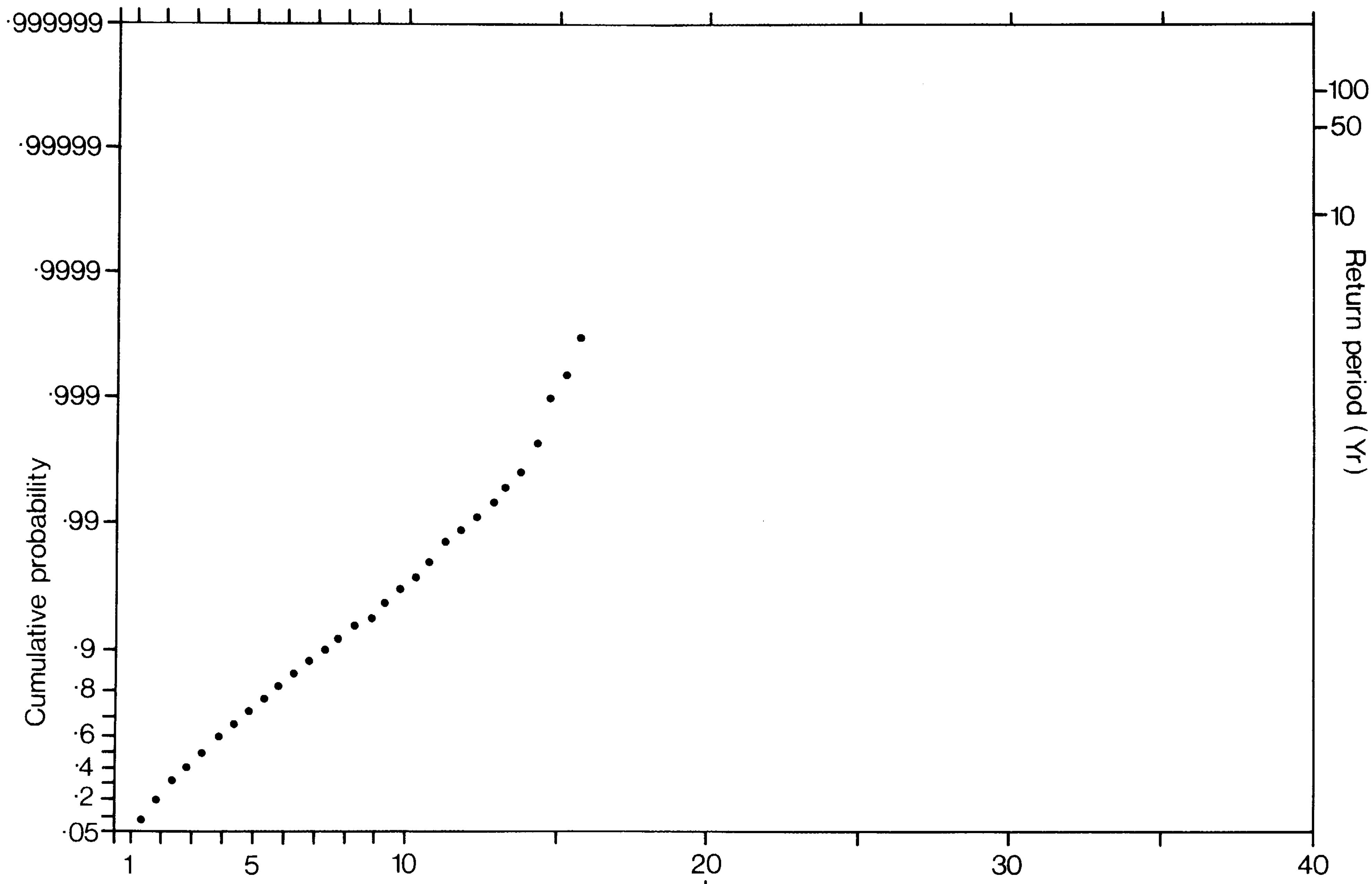

Cumulative distribution of H_{max} (3hr) Gumbel I scale *Jul 72 - Jun 73*

Fig. 33

SS

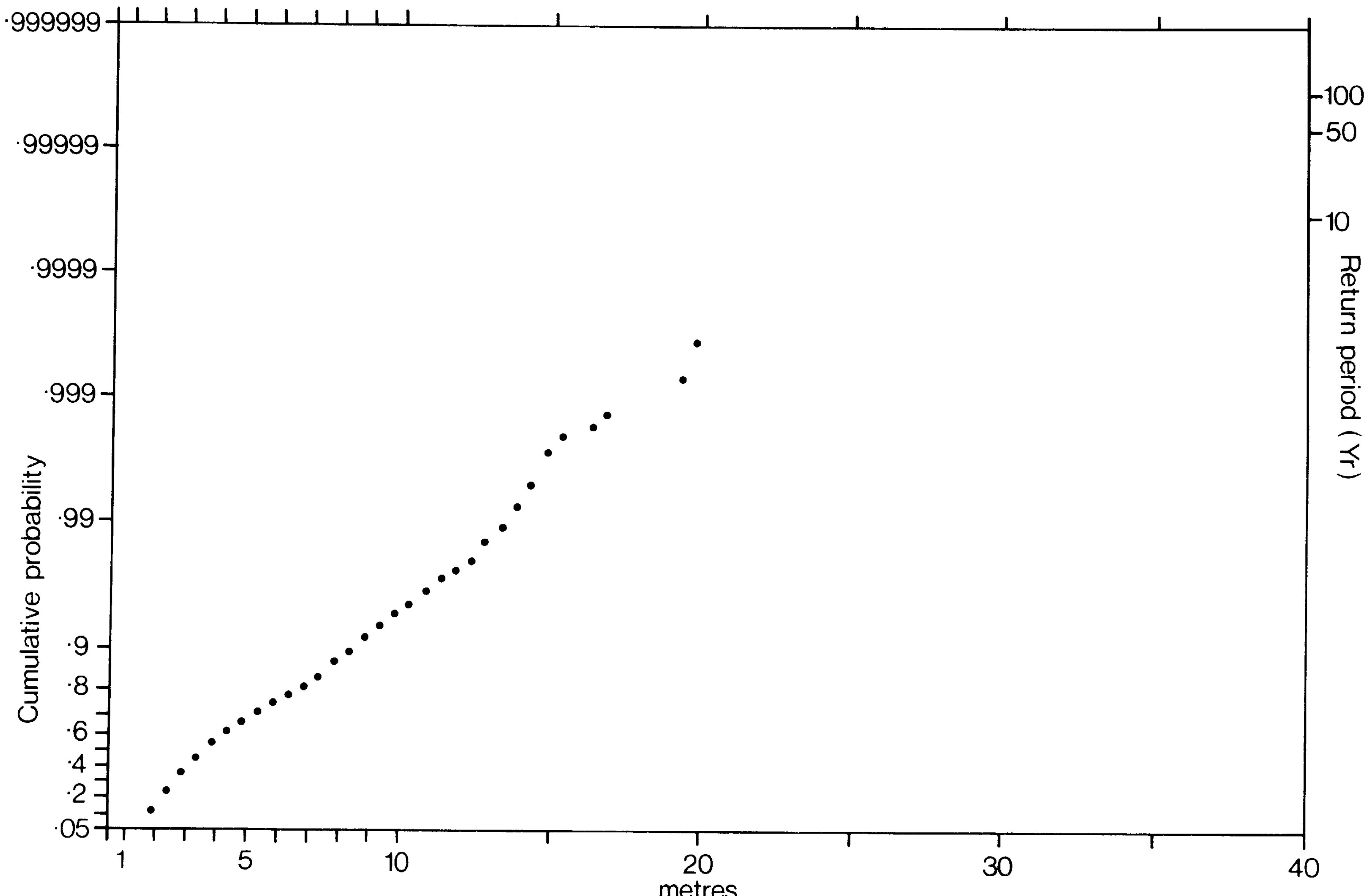

Cumulative distribution of H_{max} (3hr) Gumbel I scale ***Jul 73 - Jun 74***

Fig. 34

SS

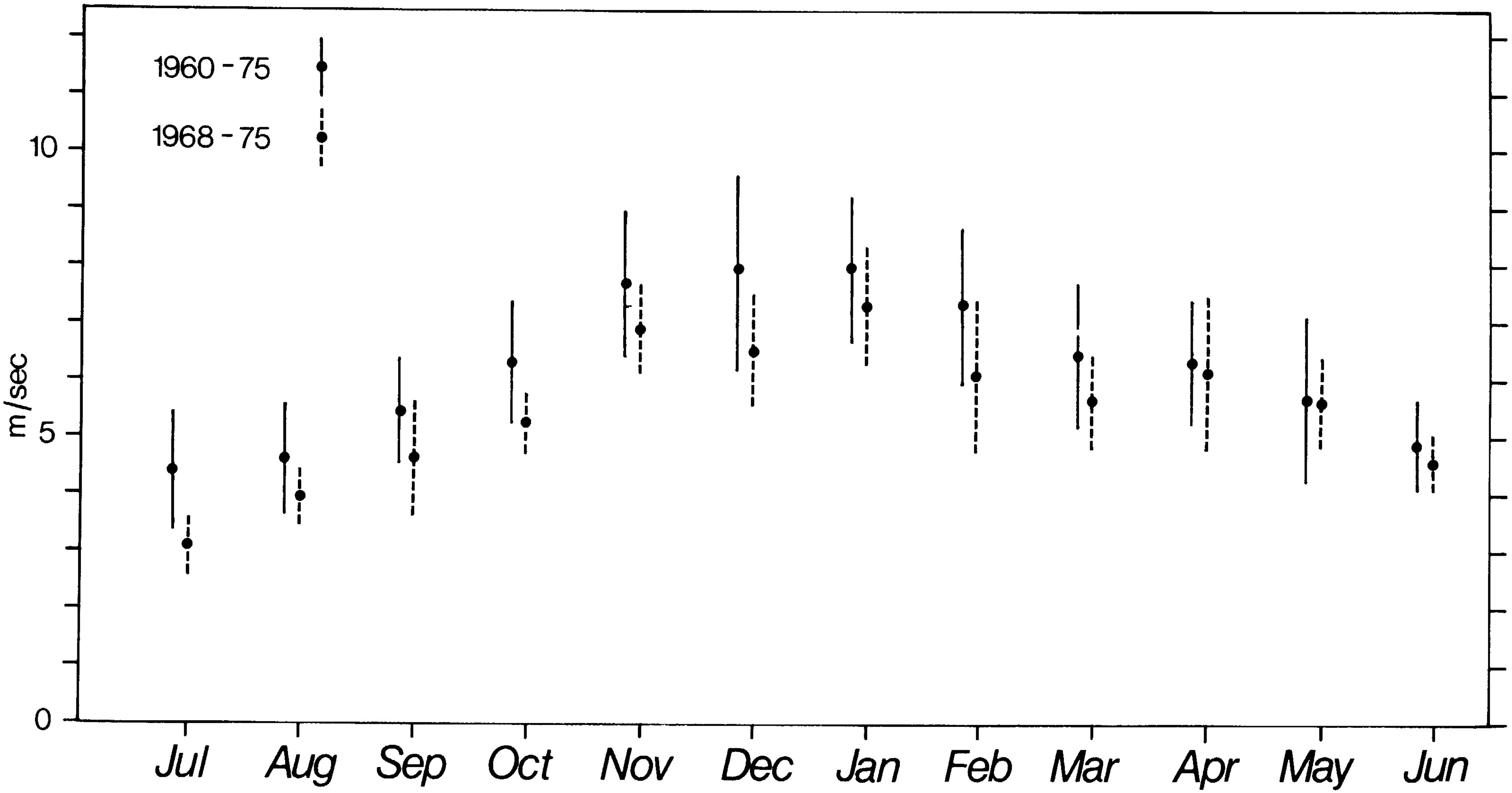

The mean and standard deviation of the average value of wind speed for each month.

Fig. 35

SS

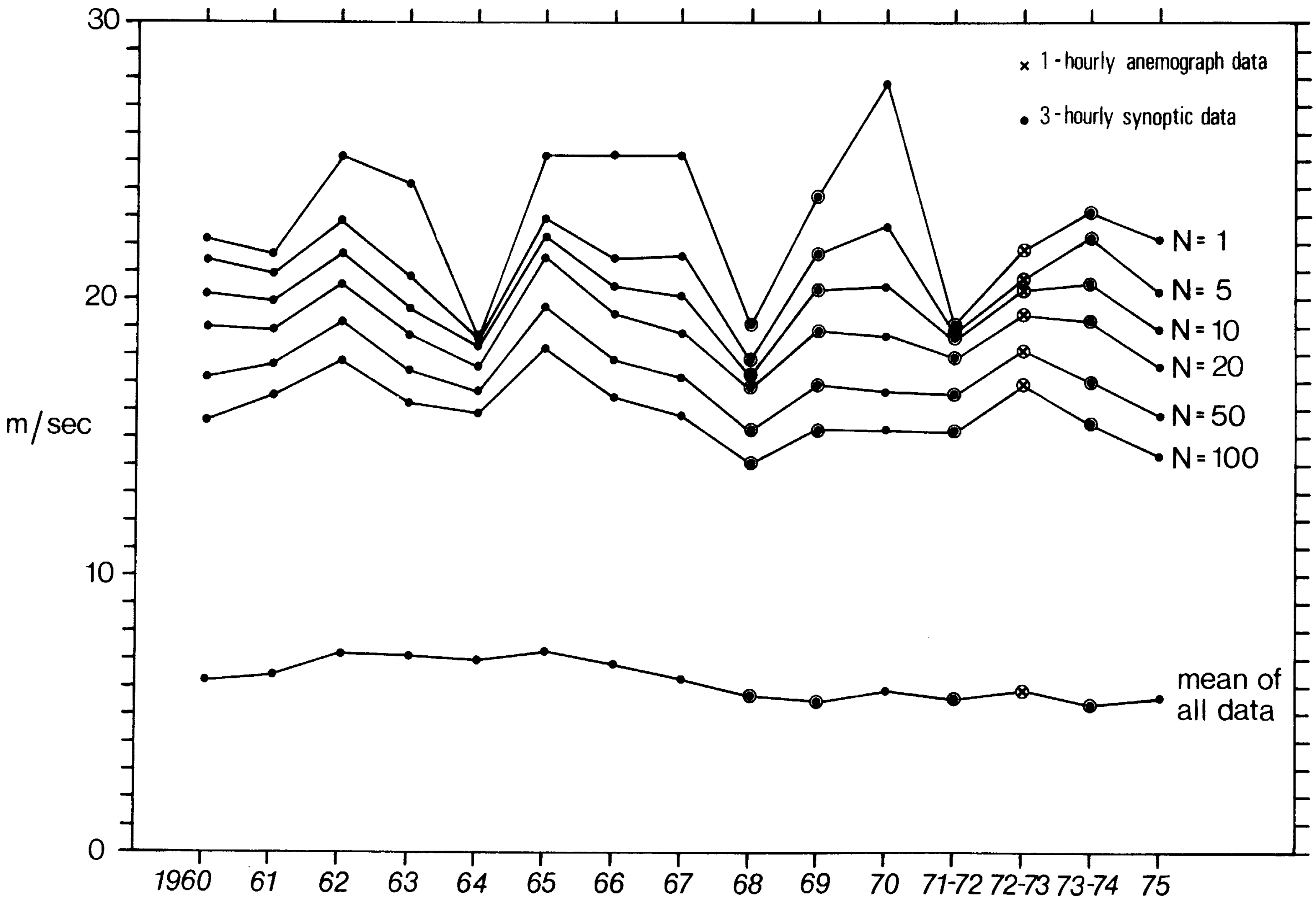

The mean of the largest 'N' values of wind speed.

Fig. 36

SS